**IMT School for Advanced Studies, Lucca**

Lucca, Italy

# The Representation of Visual Naturalistic Stimuli in Resting State Activity:

## An Investigation in the Visual and Motor Areas

## Representations at Rest

PhD Program in Cognitive and Cultural Systems

Track in Cognitive, Computational and Social Neurosciences

XXXIV Cycle

**By**

**Yara El Rassi**

**2024**

**The dissertation of Yara El Rassi is approved.**

PhD Program Coordinator: Prof. Emiliano Ricciardi, IMT School for advanced Studies Lucca

Advisor: Prof. Emiliano Ricciardi, IMT School for advanced Studies Lucca

Co-Advisor: Prof. Viviana Betti, Sapienza University of Rome

The dissertation of Yara El Rassi has been reviewed by:

Prof. Francesca Benuzzi, University of Modena

Prof. Francesco de Pasquale, University of Teramo

**IMT School for Advanced Studies, Lucca**

**2024**

# Contents

# Acknowledgments

*Sections 2.2.1 - 2.2.9 in 'methods' of Chapter 2 are borrowed with permission from:*

Betti, V., Della Penna, S., de Pasquale, F., Mantini, D., Marzetti, L., Romani, G. L., & Corbetta, M. (2013). Natural scenes viewing alters the dynamics of functional connectivity in the human brain. Neuron, 79(4), 782–797. https://doi.org/10.1016/j.neuron.2013.06.022

*Excerpts of Chapters 3 and 4 can be found in the following publications:*

El Rassi, Y., Handjaras, G., Leo, A., Papale, P., Corbetta, M., Ricciardi, E., Betti, V. (2022). A visual representation of the hand in the resting somatomotor regions of the human brain, *bioRxiv* doi: https://doi.org/10.1101/2022.04.05.486995

El Rassi, Y., Sili, D., Giove, F., Betti, V. (2023). Encoding of common grasps in the resting human brain. *OHBM 2023 annual meeting*. Encoding of common grasps in the resting human brain (uniroma1.it)

*Thank you to supervisors (Dr. Emiliano Ricciardi, Dr. Giacomo Handjaras and others), family (mom, dad, Joey, Elio, Demetrio and others), and friends (Dila, Lucas, Nat, Greg, Katia, Ari, Samoura, Mario, Poppy , Ottavia, Matteo, Peter, and others).*

# Vita

| | |
|---|---|
| Nov 11, 1994 | Born, Ajaltoun, Lebanon |
| Nov '18 | IMT school for advanced studies, Lucca<br>MOMILAB - MOlecular Mind LABoratory<br>*PhD in Social, Cognitive, and Computational Neuroscience* |
| Jun '22 - Jun '23 | Sapienza University of Rome<br>CosyncLab IRCCS Fondazione Santa Lucia<br>*Research Fellowship* |
| Sep '16 - July '18 | University of Trento<br>Melcher Active Perception (MAP) lab<br>*Master's in Neuroscience* |
| Sep '12 - July '15 | American University Of Beirut (AUB)<br>*Bachelor's in General Psychology* |

## Publications

1. El Rassi, Y., Handjaras, G., Leo, A., Papale, P., Corbetta, M., Ricciardi, E., Betti, V. (2022). A visual representation of the hand in the resting somatomotor regions of the human brain, *bioRxiv* doi: https://doi.org/10.1101/2022.04.05.486995

2. El Rassi, Y., Sili, D., Giove, F., Betti, V. (2023). Encoding of common grasps in the resting human brain. *OHBM 2023 annual meeting*. Encoding of common grasps in the resting human brain (uniroma1.it)

## Contributions

1. Always in sight: a visual representation of the hand in the resting sensorimotor regions of the brain, *Organization of Human Brain Mapping*, Glasgow, Scotland, 23 Jun '22

2. Representation of hand shape in the human resting state activity, *Congresso Nazionale SIPF*, online, 20 Nov '20

## List of Figures

## Abstract

Resting state is characterized as an offline period, during which the eyes may be either open or closed. In this disengaged state, one's system operates independently of external input or feedback, and by definition, relies on an internalized model of the world. Literature shows that resting state activity may reflect the statistics of the natural environment, but also the unique individual biases, and is possible to be reshaped over time. This is highlighted by studies that show that resting state fluctuations maintain traces of everyday activity; but how are these representations extracted, how stable are they, and to what extent are they malleable? To answer that we need to understand: 1) How is our system structured to maintain regularities? 2) How are they integrated in an internalized model? 3) How do low frequencies fluctuate when detecting an error? The main aim of this thesis is to understand how natural information is represented in resting state. The working model is that (1) naturalistic information is processed along a hierarchy in time and space to code higher level information that is low dimensional and sparse (chapter 2). 2) This information is then maintained in resting state in a generic form (chapter 3). 3) This is achieved because low frequency fluctuations are adapted to naturalistic statics, and hence are altered in otherwise unexpected situations (chapter 4). We examined the functional connectivity (FC) of MEG signal changes in the visual (VIS) and dorsal attention (DAN) networks during the observation of naturalistic videos, by comparing them to a pretrained convolutional network. We reveal distinct temporal dynamics in processing low and high-level features. Low-level features are immediately and abundantly represented, while high-level features exhibit a delayed and scarce representation, potentially storing information in a generic form (chapter 2). For instance, we find that the BOLD multivoxel spatial representation of a still hand, controlled for low-level features, is coherent with the spatial representation of the resting somatomotor area, as opposed to another object such as a food item (chapter 3). We suggest that the representations during resting states may contribute to the goal of interacting with the environment. This is enriched by our final findings; the multivoxel spatial representation of observing common movements aligns more coherently with resting somatomotor patterns as opposed to uncommon (chapter 4).

# Chapter 1

## Introduction

## 1.1. Background

*1.1.1. Definition*

As adaptive beings, an important skill to master is the ability to predict our next move, a task facilitated by learning the rules or regularities of our environment. In other words, by learning regularities, we are able to deal with future occurrences with a higher predictive efficiency. This requires an engagement with external input, but our system is also often disengaged; for example while imagining future scenarios or during sleep. So the brain can have dual modes, one engaged and another disengaged. The engaged mode interacts with the environment and constant input allows the system feedback to correct any prediction errors. In the disengaged mode, the system is by definition independent of external input or feedback. This assumes an internalized model of the world. For a system to be disengaged but still maintain activity, it must have internal resources or mechanisms that allow it to be self-organized (Buzsáki, 2019). Such models have been extensively studied during sleep and memory (Simon et al., 2022), and only recently, during resting state (Snyder & Raichle, 2012). Resting state is defined as an offline period with eyes either open or closed. For example, when detached from the world, a brain can come up with 'what if' scenarios that allow the anticipation of consequences of actions without even performing them. Internalized self-generated models are also referred to as spontaneous activity. In this thesis, the terms internalized model, resting state and spontaneous activity are used interchangeably to refer to an offline rest period.

Resting state experiments aim to capture the properties of endogenously generated (spontaneous or intrinsic) neural activity, unlike event-related studies, which focus on measuring evoked or induced responses. However, resting state studies lack the control typical in cognitive neuroimaging. Moreover, during quiet wakefulness, humans have stimulus-independent thoughts, but the cognitive content of these thoughts is not easily related to objectively measurable fMRI

responses (Gruberger et al., 2011). But it is important to note that unconstrained cognition alone does not account for the majority of intrinsic activity. Imposed tasks with constrained thought evoke responses modest in magnitude compared to intrinsic activity (Raichle et al., 2006), so there is no reason to think that unconstrained thought requires more energy. Moreover, resting state activity persists during slow wave sleep and anesthesia (Samann et al., 2011). This suggests that factors beyond unconstrained cognition contribute significantly to intrinsic activity.

*1.1.2. History*

Thomas Huxley and George Bishop were the first to understand the significance of patterned nervous activity. Huxley, examining crayfish (Huxley, 1884), highlighted how organized behaviors could occur without the need for ongoing neural activity. In 1933, Bishop observed cyclic changes in rabbit visual cortex excitability, recognizing the brain's response modulation by fluctuating endogenous activity (Bishop, 1993). Hans Berger's 1929 human EEG recordings connected mental activity with continuous cortical activity (Berger, 1929). Post-World War II, the advent of electronic computers allowed the development of Event-Related Potential (ERP) recording, revealing reproducible waveforms from ongoing EEG. Metabolic investigations by Seymour Kety in 1948 showcased the brain's high energy consumption during the resting state (Kety & Schmidt, 1948). Regional oxygen availability was measured through electrodes on the cortex of experimental animals and epilepsy surgery patients, revealing slow variations and stimulus-induced increases. Then in the 1980s, PET scans demonstrated local changes in blood flow related to glucose consumption during brain activity (Fox, 1988). Speculation still surrounded the origin of these oxygen waves and whether they only reflect capillary opening and closing. The metabolism hypothesis only gained support when it was shown that oxygen waves reflected regional fluctuations synchronous in homologous regions of both hemispheres. The relationship between these spontaneous blood flow and oxygen availability waves and electrical activity patterns in experimental animals garnered significant interest.

Bharat Biswal and Antal Hudetz, acknowledging this legacy, conducted a seminal experiment on resting-state fMRI correlations (Biswal, 1995). Resting state fMRI, known for slow BOLD signal fluctuations, was initially regarded as noise but was later demonstrated

to have neural origins by Biswal and colleagues (1995), showing temporal correlations within the somatomotor system. The neuroscience community was slow to acknowledge this, emphasizing non-neuronal sources of correlated fMRI signals. Skepticism regarding the biological significance of resting-state BOLD correlations prevailed initially, with most studies using short TRs to reduce physiological pulsation impact (Snyder, 2012). Despite initial skepticism, studies that included a resting state revealed surprising task-induced activity decreases, leading to the discovery of the Default Mode Network (DMN) (Raichle et al., 2001). The importance of resting state BOLD signal correlations became evident when Michael Greicius and colleagues depicted the Default Mode Network (DMN) using a seed region in the posterior cingulate cortex (Greicius, 2003). Similar patterns of resting state coherence have since been observed in various cortical systems and subcortical connections, underscoring the biological relevance of resting-state fMR.

*1.1.3. Importance*

The importance of resting state can be highlighted with three main observations: the existence of resting state networks (RSNs), the metabolic cost at rest, and interindividual variance with clinical implications.

1) Over the last two decades, an increasing number of studies have demonstrated that spontaneous brain activity, i.e., activity that is not evoked by stimuli, tasks, and responses, does not reflect random noise as postulated by early neurophysiological studies (Shadlen & Newsome, 1998). Instead, research found that the low frequency (0.1 Hz) fluctuations of the blood oxygen level-dependent (BOLD) signal are highly structured in space and time (Raichle et al.,2001; Fox and Raichle et al., 2007). These findings led to other experiments that show that spontaneous and task evoked activity are correlated and their coherence increases with development (Lewis, 2009). The first systematic investigation addressing the spatiotemporal structure of the spontaneous activity focused on the hand region of the primary sensorimotor cortex (Biswal et al., 1995). Through interregional correlations at rest, or resting-state functional connectivity, authors found that the topography of the sensorimotor areas is similar to that evoked by finger movements (Biswal et al., 1995). Several other studies have since confirmed this result, revealing functionally related brain regions or resting-state networks – RSNs - that exhibit correlation of

intrinsic fluctuations in the cortex (Deco et al., 2011; Yeo et al., 2011). RSNs are divided into sensory networks that include the visual, auditory and sensorimotor systems, and cognitive networks that include the dorsal and ventral systems. The areas are functionally connected and therefore can create functional parcels of the brain (Yeo et al., 2011). fMRI neurophysiological correlates spam from 0.1 to 1 Hz in alpha and beta band limited power fluctuations (Hutchinson et al., 2013). The anatomical/structural connectivity is highly correlated with the functional topography at a group level (Deco et al., 2013) and the topography of these networks is resilient across different levels of consciousness and is similar to task-induced patterns (example Betti et al., 2013; Cole et al., 2014). RSNs can be classified at a static level, however their dynamic variation over time has also been linked to changes in cognitive states (Hutchinson et al., 2013). Specific tasks can change the scaffolding of RSNs. For example, after a long training on a new task, few pathways will have different levels of intrinsic correlation, as cognitive tasks will change a (relatively small) number of synapses and pathways (Albert et al., 2009; Lewis et al., 2009). Miller (2014) investigated the resting V1 of wake mice using two-photon calcium imaging. They found that independent neurons flexibly join ensembles of neurons and expand the potential of the circuit. They concluded that visual stimuli recruit intrinsically generated ensembles to create visual representations. Therefore, blood oxygenated signals in fMRI measuring infra-slow frequencies without external input are now accepted not as noise given the fact that they are correlated in large networks that are task related (Fox & Raichle, 2007).

2) Though this ability is greatly useful for survival and efficiency, it is also costly from a metabolic and energetic perspective. In fact spontaneous activity is characterized with infraslow activity in the brain (Mitra et al., 2018), and it consumes most of the energy budget of the brain (Tomasi, 2013). The brain's high energy consumption is essential for its functions, and understanding how this energy is used during resting state can provide insights, especially for studying disorders related to metabolism. The brain represents 2% of total body weight yet has an energy consumption of 20% (Kety & Schmidt, 1948). Of that, about 60-75% is consumed in electrochemical signaling (Mitra et al., 2018). Interestingly, only 10% of the energy budget is consumed during firing of sensory processing while the rest is concentrated from the activity of neurons in the infra-slow frequency range. Mitra and colleagues (2018) investigated spontaneous brain activity, particularly

infra-slow fluctuations, through imaging techniques like functional magnetic resonance imaging (rs-fMRI) in humans and optical imaging in mice. Despite the widespread use of rs-fMRI, the underlying biology of spontaneous patterns in BOLD signals and infra-slow brain activity remains unclear. The conventional view suggests that infra-slow phenomena are a summation of fast, local neural activity. In contrast, the study explores the possibility that infra-slow activity is a distinct brain process with its own principles, traveling through the cortex along specific trajectories. The study aimed to differentiate infra-slow activity from delta activity, examine if BOLD signals correspond specifically to infra-slow neural activity, explore potential behavioral correlates, and investigate whether infra-slow activity exhibits laminar specificity in the cortex. The findings reveal that infra-slow activity indeed follows distinct spatio-temporal trajectories in the mouse cortex, separate from higher frequencies (Mitra, et al., 2018). In order to understand the energy consumption of this activity, Tomasi and colleagues (2013) used a combination of PET imaging to measure glucose metabolism and MRI to analyze functional connectivity in 54 healthy individuals at rest. They showed that glucose metabolism (CMRGlu) was highest in specific brain regions, such as the cerebral cortex, and that these regions also exhibited higher amplitudes in resting-state fMRI signals. The study found a linear association between glucose metabolism and the amplitude of resting-state fMRI signals. Additionally, the researchers explored the relationship between glucose metabolism and the degree of functional connectivity by measuring the number of connections a brain region has with others. They observed power scaling, suggesting that higher glucose metabolism is associated with increased functional connectivity. The study suggests that a considerable proportion of energy (70%) is dedicated to maintaining baseline functions and supporting the intrinsic connectivity and communication between different brain regions during resting state (Tomasi et al., 2013).

3) The importance of the study of spontaneous activity has been also shown in literature studying individual variability. Spontaneous activity changes with learning (Lewis CM et al., 2009; Fiser J et al.,2004), predicts predispositions (Baldassarre et al., 2012), and reflects individual cognitive differences (Smith et al., 2015; Finn et al., 2015) and abnormalities (Baldassarre et al. , 2016). In one review (Baldassare, 2016), the authors focus on the challenge of identifying neural mechanisms underlying behavioral deficits after a brain stroke. The

findings highlight two main patterns of functional connectivity changes after focal brain lesions: a reduction in interhemispheric connectivity and an increase in intrahemispheric connectivity between normally anticorrelated networks. The review emphasizes the behavioral specificity of these connectivity changes, connecting deficits in specific domains to corresponding resting state networks. Additionally, it discusses the restoration of prestroke functional connectivity patterns during behavioral recovery. The authors propose that investigating network changes can provide insights into neural mechanisms post-stroke and suggest resting-state functional connectivity as a valuable tool for clinical diagnosis, recovery tracking, and rehabilitation. This is because contrary to the traditional view of the brain as a passive analyzer of sensory stimuli, the authors suggest that spontaneous cortical activity actively maintains ongoing representations related to expected sensory stimuli, prospective motor responses, and prior experiences. The review also links resting-state functional connectivity to rehabilitation interventions, such as transcranial direct current stimulation (tDCS) and intermittent theta-burst stimulation (iTBS). In conclusion, understanding individual variability in spontaneous brain activity patterns may contribute to personalized treatments and early diagnosis after stroke.

In fact, another study (Finn et al., 2015) highlights that an individual's functional brain connectivity profile is unique and reliable, akin to a fingerprint. The authors demonstrate the near-perfect accuracy of identifying individuals based solely on their connectivity matrix. While there is a general blueprint shared across individuals, the functional organization within each person is idiosyncratic, relatively robust to changes in brain state, and provides meaningful information beyond the common template. The study also shows that this individual variability is relevant to differences in behavior, as connectivity profiles can predict intelligence. The frontoparietal networks, involved in cognition and cognitive control, are particularly distinguishing of individuals and predictive of behavior. The results suggest the potential for personalized educational and clinical practices using fMRI-based connectivity "neuromarkers" to improve outcomes. The study emphasizes the importance of analyzing individual fMRI data, moving beyond population-level inferences to explore unique functional organizations and their relationships to behavioral phenotypes in both health and disease.

Interestingly researchers have even investigated the relationship between the functional connectomes of individual subjects and 280 behavioral and demographic measures in 461 participants from the Human Connectome Project (Smith et al., 2015). Using canonical correlation analysis (CCA), they identified a strong mode of population co-variation, revealing a single "positive-negative" axis that links lifestyle, demographics, and psychometric measures to a specific pattern of brain connectivity. The analysis suggests a one-dimensional axis resembling a general intelligence factor, incorporating aspects of real-life function such as education, income, and life satisfaction. The findings highlight a unique mode of positive brain function, providing insights into the underlying biology of population variability in behavioral and brain connectivity measures.

*1.1.4. Role/Function*

Literature shows that infra-slow frequencies have a distinct organization with its own function and neurophysiology (Breakspear, 2017). But even if resting state fluctuations are an independent neurophysiological process, their role or function remains under debate. One explanation, enforced by the similarity of rest and task topography, is that resting state is reflecting the history of coactivation of brain networks, that creates a prior architecture for the subsequent recruitment of task networks. In other words, intrinsic activity could be molded through environmental statistical learning, creating priors that affect further task-driven activity (Betti et al., 2018). In predictive coding, top-down information helps predicting lower level incoming stimuli that then can be corrected from the incoming stimuli, if there are predictive errors. If there are no external stimuli, then prediction errors are not elicited. During this time, the brain might be reiterating the brain's priors (Lewis et al., 2009; Fiser et al., 2010; Stoianov et al., 2020).

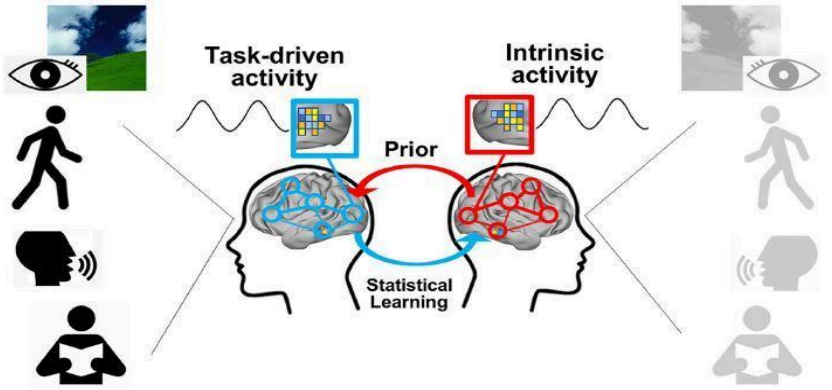


**Figure 1 Priors** Intrinsic activity is molded through environmental statistical learning creating priors that affect further task-driven activity (Betti et al., 2018).

There are 3 sets of experiments that best support the framework of resting state functioning as a prior. The first shows that spontaneous activity changes over short and long term periods, the second shows how it affects perception in vague situations, and the third shows that it adapts to the natural but not artificial environment.

One set of literature has used a design of rest-task-rest, with the second resting state session either immediate (for example Barnes et al., 2009) or after a long training (Lewis et al., 2009; Ma et al., 2011; Taubert et al., 2011). Resting state activity is altered for a few minutes after a 1-back working memory task, without explicit memorization (for example Barnes et al., 2009). This finding highlights how spontaneous activity reflects or has traces of current or recent experience, even if it is passive. Then other experiments with a rest-task-rest design show long term effects of visuospatial training (Lewis et al., 2009) or motor training (Ma et al., 2011) on intrinsic connectivity, even changing structural connectivity after extensive training (Taubert, 2011). Together, these experiments show how everyday tasks mold spontaneous activity that is dynamically altered both with immediate and long term experiences.

This literature is supported by other experiments that studied resting state over development. For example Berkes (2011) showed that internal models are optimally adapted to the statistics of the environment by

analyzing the activity in the visual cortex of ferrets throughout their development. The authors found that spontaneous and evoked activity increased in similarity with age. Crucially, this observation was specific to evoked responses of natural scenes not artificial objects, showing the adaptation of the internal model to natural stimuli. Similarly, Strapini (2019) showed that resting state fluctuations reflect the statistics of habitual cortical activations during real life. The authors referred to this phenomenon as spontaneous trait reactivation (STR). Resting state patterns and evoked connectivity patterns of natural stimuli were significantly more correlated than rest patterns and evoked connectivity patterns of artificial stimuli. Therefore, spontaneous activity reflects the statistics of habitual cortical activations during real life (Strappini, 2019) and increases in similarity with evoked activity with age (Berkes et al., 2011). This observation is specific to evoked responses of natural scenes not artificial objects (Berkes et al., 2011; Strapini et al., 2019; Kim et al., 2020).

This malleable internal model is particularly important in vague situations when an individual is high on sensory uncertainty, as they can use prior knowledge to predict and interact with the environment. Experiments with perceptual ambiguity or near threshold stimuli show how the internal model can help with perceptual influence in ambiguous real life situations. For example the connectivity from the fusiform face area (FFA) to early visual area (V1) in the pre-stimulus period predicts when subjects will perceive a face when viewing the Rubin vase/face illusion (Rassi, 2019). This shows how spontaneous activity can affect visual perception. Hesselmann and colleagues (2008) instead looked at motion-sensitive areas. They presented near threshold dots calibrated to each participant and asked them whether they perceived random or coherent motion. They found a higher activity in the pre-stimulus interval when subjects reported perceiving coherent as opposed to random motion. In summary, 1) spontaneous activity biases perception and affects behavior in ambiguous situations. 2) This relationship is specific to brain sensitive areas. This idea is further supported by Kim and colleagues (2019) who found that patterns of spontaneous activity were coherent across regions, but varied within one region to the extent that they positively or negatively matched the regions' preferred stimulus evoked patterns.

## 1.2. Representational model

The previous literature allows us to make a set of observations: resting state activity should correspond to average training in daily life, reflects the statistics of the world, but also the unique individual biases, and is possible to be reshaped over time. Therefore, spontaneous activity is highly dependent on the statistics of the natural environment, but how does it represent that information? Resting state priors could be in the form of representations more similar to distributions of data rather than specific data points allowing the optimization of models. This generic information would have to summarize a big amount of information or natural statistics so they are more likely to be low-dimensional states. This low dimensionality is already shown in monkeys and human fMRI response to movement. For example, Churchland and colleagues (2012) showed that the principal component that accounts for both rhythmic (walking) and non-rhythmic (reaching to grasp) motion is a phasic oscillatory activity regardless of the kinematics of the movement. In other words, the mechanisms underlying different kinds of movement can be explained with the variance of 1 principle component. Semantic stimuli (Huth et al., 2012) can also be grouped in a semantic space that accounts for diverse objects and action verbs, and understanding of 3D surfaces requires the understanding of distances and openness only to be able to reconstruct the scene from neural brain activity (Lescroart & Gallant, 2019). Finally, we see this low dimensionality also present in resting state: for example in the visual cortex the resting data is more similar to categories rather than specific exemplars (Kim et al., 2020), and common movements are more coherent with rest than uncommon (Livne T et al., 2020). Such a generic model is useful because it is more flexible to explain incoming data. For example, spontaneous activity is not limited to the main function of one cortex, patterns are not motor specific in the motor cortex or sensory specific in the sensory cortex. The patterns would have to be general patterns that explain the natural world.

A similar mechanism, sparse coding, has already been proposed in the brain: sparse coding is a mechanism that efficiently represents the whole of the information with lesser variables (Beyeler, 2019). For the brain to take in all information with its high dimensionality, there would have to be a lot of linear and non linear computation and cross talk in order to explain the information, also in relation to history/experience and context. On one extreme, each node

could be assigned to every piece of information possible, but that would require a lot of nodes and is anatomically limited, on the other extreme the average population activity could explain the information, but there would be a lot of crosstalk because all neurons are involved in all contexts. So how is this natural information collected and coded? One way to solve this problem is through dimensionality reduction sparse coding, where neural activity represents information with a smaller population, thereby reducing activity (Cunningham, 2014). When looking at the shared activity of a population, some nodes could be affected because they are not independent of the nodes next to them. In dimensionality reduction, this shared activity is elucidated to allow a proper explanation of population activity. Ultimately, this allows the explanation of information with less nodes than all the population nodes (Cunningham, 2014). In the brain model, the brain would reformat sensory data maintaining full representation with the smallest possible number of neurons. It does so by adapting to the statistics of the inputs allowing neurons to become selective to particularly recurring patterns. The reason this principle has great appeal is because it lends an explanation to learning and creating associations or bridging in higher order areas, by still explicitly maintaining the structure and features of the images (Beyeler, 2019). This method is also thought to have other advantages like better memory storage, clear representation of natural signals, easy interpretation of complex data, and energy efficiency (Olshausen et al, 2004). Olshausen and colleagues (2004) show evidence from experiments supporting the use of sparse coding in various sensory systems across different animals highlighting observations in the vision system of primates.

Even if sparse coding is one of the efficient coding models of the brain, its effectiveness depends on various factors, including the coding capacity (signal-to-noise ratio) and the decoding lag (the time delay for prediction). The optimal efficient coding model for predicting the future differs based on these parameters (Chalk, 2018). Chalk and colleagues (2018) show that the optimal neural code depends on whether the goal is to recover information from the past or predict future stimuli. The study emphasizes the tradeoffs that sensory neurons face, exploring the consequences of optimizing neural responses for predicting the future compared to efficiently encoding past inputs. This exploration leads to qualitatively different predictions for how neurons respond to natural visual stimuli. Sparse coding, which is often associated with efficiently representing stimuli with a sparse latent

structure, is found effective when the goal is to maximize information about past inputs (encoding the past) and is observed at low noise (high capacity). However, it is not the optimal strategy when the objective shifts to efficiently predicting the future. When there is a tradeoff between maintaining a sparse code and responding quickly to stimuli within the receptive field, neurons might become selective for motion speed but not direction (Chalk, 2018).

Despite being discussed for a long time, researchers have only recently started exploring sparse coding in real-world situations using natural stimuli to understand how it works in specific parts of the brain. Empirical investigations into sparse coding have gained momentum only recently, with the need for studies employing ecologically valid stimuli to understand its utilization in specific neural regions.

## 1.3. Aims and Hypotheses

Literature shows that resting state fluctuations maintain traces of everyday activity, but how are these representations extracted, how stable are they, and to what extent are they malleable? To answer that we need to understand: 1) How is our system structured to maintain regularities? (chapter 2) 2) How are they integrated in an internalized model? (chapter 3) 3) How do low frequencies fluctuate when detecting an error? (chapter 4). The main aim of this thesis is to understand how natural information is represented in resting state. The working model is that 1) naturalistic information is processed along a hierarchy in time and space to code higher level information that is low dimensional and sparse.2) This information is then maintained in resting state in a generic form. 3) This is achieved because low frequency fluctuations are adapted to naturalistic statistics, and hence are altered in otherwise unexpected situations.

In this thesis we use several neuroimaging techniques (MEG and fMRI) along with different machine learning methods. It is important to highlight that the choice of neuroimaging machine depends on the aim of the study and hence its design. fMRI relies on changes in blood oxygenation levels to infer neural activity, offering high spatial resolution but with a much slower temporal resolution in the order of seconds. MEG instead, a more direct measure of brain activity, measures the magnetic fields generated by neural activity, providing high temporal resolution on the order of millisecond. While MEG excels at capturing the rapid dynamics of neural processes, its

spatial resolution is limited, making it difficult to localize activity within deep brain structures. fMRI on the other hand can provide insights into both cortical and subcortical brain regions, allowing for a more comprehensive understanding of brain function. Despite their differences, using these complementary techniques allows us to gain a more comprehensive understanding of brain function by integrating findings.

In the first experiment we characterize how MEG functional connectivity is affected in the visual stream along the dorsal pathway during natural video viewing. In natural viewing, we extract temporal regularities through statistical learning and build temporal structures with schemas that influence the interpretation of new information acquired – this allows one to predict upcoming events over long timescales (Gilboa & Marlatte, 2017; Van Kesteren et al., 2012) . The brain contains a hierarchy of regions that respond to information over varying timescales (Chaudhuri et al., 2015) and low level events are gradually integrated into minutes of long situation level events using a multistage nested temporal chunking (Baldassano et al., 2017). In the time domain, cognitive processes rely on the accumulation of information allowing the processing of information to unfold in a temporal hierarchy where different cognitive processes unfold over different delays (Hasson et al., 2008). A body of literature has investigated naturalistic temporal structure in the human visual system relying on comparing intact movies with scrambled versions to understand the integration of information over time using fMRI (Hasson et al., 2008; Lerner et al., 2011; Aly et al., 2018) or ECOG (Honey et al., 2012). Findings show that sensory areas track instantaneous physical parameters and are unaffected by scrambling so they have short processing timescales. Instead higher order areas are sensitive to temporal context and extend tens of seconds along the processing scales (Hasson et al., 2015). In the first experiment, we characterize how the brain processes incoming stimuli through the visual system over long 40 second intervals. We correlate MEG data of natural movie watching to a deep neural network fed the same movie. The visual system in the brain hierarchically processes characteristics of images through the dorsal visual flow. Deep Neural Networks (DNN) confirm the existence of a gradient in complexity of neural representations across visual areas (Guclu & van Guralerven, 2015): early visual areas like V1 process low level features like luminance and contrast, and higher parietal and temporal regions process high level

features like categories (Cichy et al., 2016). Recent advances in feedforward quantitative models like DNN and CNN have helped us capture and confirm this hierarchical multi-stage complexity of the spatio- temporal dynamics of the visual stream (Guclu & van Guralerven, 2015). Here we utilize a pre-trained CNN and correlate it to MEG data in order to understand how the connectivity changes in the visual stream along the dorsal attention network. Along the hierarchy, we expect changes both in time and in space. We expect high level features to be processed at later time intervals than low level features, but to be represented sparsely in a reduced dimensionality as opposed to low level features.

In the second experiment, we test using fMRI the generic representation of the hand, the main effector that we use to interact with our environment. As humans evolved, the thumb has become one of our most distinctive features (Wilson et al., 1988). The study of the representation of hands in the brain is ever more important for both clinical and technological purposes. A rich literature is dedicated to the study of the kinematic and neuroimaging data describing hand representations in the brain: Recent research shows that a number of synergies with low-dimensionality of hand movements are invariant across subjects with a fixed cortical representational structure (3 to 6 principle components explain 80% of variability) (Belic & Faisal et al., 2015). Moreover, plastic changes can be predicted by natural hand usage statistics (Leo et al., 2016). When investigating fine grain digit somatotopy in the somatosensory hand area at the level of individual human participants, Kolasinski and colleagues found stable and reproducible maps of individual digits in S1 (Kolasinski et al., 2016). Ejaz and colleagues (2015) showed that neurons in M1 encode coordinated finger movements, and cortical stimulation evokes movement of several fingers simultaneously as in natural hand use. Here we ask if the representation of the hand is also maintained at rest: the hand being an active sensory organ, naturally has internal representations at rest that resemble those during touch and action in the somatomotor area (Biswal et al., 1995). But to test the generic stability of that encoded information, here we first ask, what about the passive representations of visually presented static hands in the somatomotor cortex at rest?

In the third experiment, we explore how the visual and motor areas in the action observation network detect error and how that alters

low frequency fluctuations. Visually guided motion is important for coordination and control of individual fingers. According to animal models, the anterior intraparietal sulcus that processes object features, sends information to the ventral premotor that elaborates visual and space information and sends a motor representation to the dorsal premotor. The dorsal premotor then updates and reconfigures the information to send it to M1 for execution (Castiello & Begliomini, 2008). These same areas are implicated in the action observation network (AON). The AON can be defined through a two path model with separate action comprehension mechanisms. The ventral system is the signal sent from V1 to the temporal area for object recognition, and the dorsal is the signal sent from V1 to the parietal for kinematic configuration. These two systems interact through the ventral dorsal pathway, but there also exists a separate dorsal-dorsal pathway that computes error (Amoruso, 2020). However, even if guided motion and action observation activate the same systems, they do not respond equally to error. After error detection in execution, there is an increase in inhibitory activity, and decrease in facilitation, however during observation after the detection of error, there is a decrease in inhibition, and an increase in facilitation (Cardellicchio, 2018). This is more in line with a predictive coding account, where the detection of error as a result of the mismatch between what is expected and what is observed causes an increase in activity. When watching naive subjects perform a complex novel action, there is an increase in activation in the dorsal parietal vs when observing an expert performing the action without error (Errante, 2019). In resting state literature, abundant work shows similarities between task-driven and intrinsic (low frequency fluctuations(LFFs)/ resting state) driven activity. But how exactly do task-related functional connectivity (FC) of LFFs get modulated in relation to error, and what is the significance of this information?

# Chapter 2

## Functional connectivity changes in natural viewing depending on low level or high level features: an MEG study

## 2. 1. Introduction

The visual stream represents increasingly more complex features: whereas earlier visual areas have small receptive fields (RFs) and respond to lines or edge orientation, later areas have bigger RFs (Livingstone & Hubel, 1988). Similarly in the time domain, cognitive processes rely on the accumulation of information allowing the processing of information to unfold in a temporal hierarchy where different cognitive processes unfold over different delays, or temporal receptive windows (TRWs) (Hasson et al., 2008). If the TRW in an area reflects the area's functional role, then TRWs in higher areas should be bigger, allowing the processing of information that unfolds over time (Hasson et al., 2008). A body of literature has investigated naturalistic temporal structure in the human visual system relying on comparing intact movies with scrambled versions to understand the integration of information over time using fMRI (Hasson et al., 2008; Lerner et al., 2011; Aly et al., 2018) or ECOG (Honey et al., 2012). Findings show that sensory areas track instantaneous physical parameters and are unaffected by scrambling so they have short processing timescales. Instead higher order areas are sensitive to temporal context and extend tens of seconds along the processing scales (Hasson et al., 2015). Here we ask how the statistics of natural visual scenes change the functional connectivity in the brain depending on low-level features (contrast-luminance) or high-level features (object recognition) of movie images in the visual network over long lags, in the alpha (8-12 Hz) and beta (15-30 Hz) bands.

Alpha- and beta-BLP connectivity are the main MEG correlates of fMRI RSNs (de Pasquale et al., 2010; Betti et al., 2013). Beta has been associated with somatomotor modulation and perceptual processing,

such as language (Weiss and Mueller, 2012), response inhibition (Fonken et al., 2016), reward processing (Marco-Pallarés et al., 2015), visual processing (Betti et al., 2018), and maintenance of the status quo (Engel & Fries, 2010). Even though its functional role is still debated, while early literature suggested that it reflects cortical idling, more recent evidence, mainly in the visual field, has showed a role in maintaining the current status quo (Jenkinson & Brown, 2011; Betti et al.,2021; Engel & Fries, 2010; Spitzer & Haegens, 2017). Alpha's role instead is gating by inhibition (Klimesch et al., 2007; Jensen & Mazaheri, 2010). In natural environments, we process all the incoming information flows through a bottleneck mechanism: feedback modulates the processing in early visual areas to boost important representations (Jensen et al., 2015; Rassi et al., 2019) and feedback is modulated by changes in neuronal synchronization (Von Stein & Sarnthein, 2000). Regions that are not involved in certain tasks are inhibited to facilitate communication in other engaged areas. By gating by inhibition alpha functionally blocks task irrelevant pathways to route information.

Recent advances in feedforward quantitative models like deep neural networks (DNNs) have helped us capture and confirm this hierarchical multi-stage complexity of the spatio- temporal dynamics of the visual stream (Guclu et al., 2015). DNNs have proved reliable for the understanding of how stimulus features of varying complexity are mapped across the cortical sheet: the gradient of complexity of neural representations across visual areas suggests that object categorization could be the guiding principle for the formation of receptive field properties in the ventral stream (Guclu et al., 2015). Lower layers have representational similarities confined to the occipital lobe of the brain, and higher layers have significant representational similarities with more anterior regions in the temporal and parietal areas (Cichy et al., 2016).

Whereas earlier studies looked at the spatial and temporal representation similarity of features along the ventral visual stream, here we take the next step utilizing a feedforward CNN to show how the statistical properties of visual stimuli affect the functional interactions and connectivity in regions along the dorsal stream in naturalistic settings. We therefore employed source level MEG alpha and beta BLP correlation to measure functional coupling over long delays in the visual and dorsal attention networks during natural movie viewing. A deep neural network comprising 7 layers was used to

model the statistical features of the natural scenes. By mapping the CNN output to the BLP functional connectivity within and between our networks of interest, we obtained correlation matrices between the BLP connectivity and the movie low level features, and matrices between the BLP connectivity and movie high level features. This allowed us to characterize the spatiotemporal variation of the biological response depending on low level features (contrast-luminance) or high level features (object recognition) of the images. We show that the graduated complexity of natural scenes captured by network layer representations not only produces modulations of activity along the visual stream, but it also modulates patterns of functional connectivity in space and time. We found that in time, low level features alter the connectivity across a spread of nodes at early latencies in alpha and are maintained for longer latencies in beta. High level features instead produced sparse responses of connectivity in both alpha and beta.

## 2.2. Methods

*2.2.1. Participants*

Twelve healthy participants (mean age 24.7, range 21–31, five females; same sample as in Betti et al., 2013, 2018) without significant psychiatric or neurologic diseases and with normal or corrected-to-normal visual acuity participated in the study. All subjects were right-handed as judged by the Edinburgh Handedness Inventory (Oldfield, 1971). The study was approved by the Ethics Committee of G. d'Annunzio University, Chieti (Italy) in accordance with the standards of the 1964 Declaration of Helsinki. Before the experiment, participants gave their written informed consent.

*2.2.2. MEG recordings*

Magnetoencephalography (MEG) data are the same as in (Betti et al., 2013, 2018), collected while subjects watched in 3 blocks 3 different sessions of the movie *The Good, the Bad, and the Ugly* of 5 minutes each. Before movie observation, each subject underwent 3 blocks of fixation ( 5 minutes each).

Data were recorded using the 153-channel MEG system (Della Penna et al., 2000) installed in a magnetically shielded room at the University of Chieti, Italy. The channels were dc SQUID integrated magnetometers arranged over a whole-head helmet surface. Horizontal and vertical electrooculogram signals, together with the

electrocardiogram (ECG) signals, were simultaneously acquired with magnetic signals and were used during preprocessing for offline artifact rejection. The neuromagnetic and electric signals were band-pass filtered at 0.16 –250 Hz and sampled at 1025 Hz. The head position relative to the MEG sensors was measured before and after each recording session through a fit of the magnetic field generated by five coils placed on the scalp. The coil positions were digitized by means of a 3D digitizer (3Space Fastrak; Polhemus), together with anatomical landmarks (left and right preauricular and nasion) defining a coordinate system. In a separate session, a 3D high-resolution T1-weighted image was recorded from each subject's head (3D MPRAGE pulse sequence, TR=8.1 ms, TE=3.7 ms, voxel size=0.938 mm X 0.938 mm X 1 mm), through a 3T MR Philips Achieva scanner installed at the University of Chieti, Italy. The MRI anatomical images were coregistered to the head position acquired during the MEG acquisition and then used to build the individual volume conductor.

*2.2.3. MEG preprocessing and analysis*

We applied an ICA approach to remove environmental and physiological (e.g., cardiac, ocular) artifacts from sensor space MEG signals and retain the brain independent components (ICs) (Mantini et al., 2011). The sensor maps of the brain IC were scaled to [-100, 100] and were then projected in the source space, represented by a 3D Cartesian grid (4 mm voxel side) by means of a weighted minimum-norm least-squares (WMNLS) estimator implemented in Curry 6.0 (Neuroscan). The noise level used by the WMNLS estimator was set to 6% of the maximum absolute value of the IC map. This value was experimentally selected from independent sets of data (dePasquale et al., 2010,2012; Mantini et al., 2011; Marzetti et al., 2013). The individual 3D grid was then projected onto the MNI 152 atlas space through SPM8 so that every voxel centroid was assigned to a set of MNI coordinates. The activity of each voxel in the grid was estimated as the linear combination of the brain IC time courses multiplied by the related weight vectors into the source space. Our analysis was restricted to alpha- and beta-BLP connectivity, the main MEG correlates of fMRI RSNs ( de Pasquale et al., 2010,2012; Betti et al., 2013; Marzetti et al., 2013). For each voxel in the MNI grid, the source space signal was filtered in the alpha (X-Y Hz) and beta (X-Y Hz) bands using separate high-pass and low-pass Chebyshev II IIR digital filters with order 10 (the order was 8 only for the high pass in the alpha band) and stopband

ripple 10 dB. The source-space MEG BLP time series were estimated as with a 150ms sliding window size at window shifts of 20ms. Because our previous study (Betti et al., 2013) showed that movie watching induces the largest modulations of the interaction strength in these two bands and at frequencies 0.3 Hz, we restricted our analysis to this slow band.

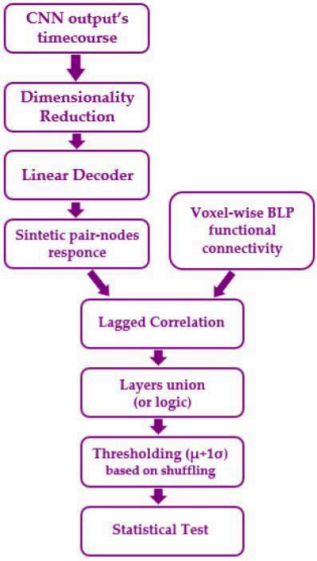


**Figure 2.1 Preprocessing pipeline** The description of preprocessing steps of CNN output and BLP FC

*2.2.4. Estimation of BLP connectivity*

The static and dynamic BLP interactions were estimated through the Pearson's correlation coefficient across 45 nodes arranged in seven RSNs (see Betti et al., 2018). However, in this study, we only focused on the Visual Network – VIS (10 nodes), and Dorsal Attention Network (6 nodes). To minimize spatial leakage effects on the estimation of BLP connectivity, we applied the geometric correction scheme (GCS) whereby leakage from a seed location is modeled on the basis of the forward and inverse models and eliminated before BLP correlation estimation (Wens, 2015; Wens et al., 2015). Because GCS may

be affected by local miscorrection effects mainly due to seed mislocalization (Wens et al., 2015), we masked out in subsequent analyses pairwise correlation values between nodes closer than 45 mm, which is compatible with simulation results reported previously (Wens et al., 2015). Accordingly, these values were removed from all the next analyses. For each run, the dynamic interaction matrices were obtained using windows lasting 10 s, sliding in 200 ms time-steps. This duration was retrieved in our previous study (Betti et al., 2013) showing that naturalistic viewing influences internodal BLP interaction for fluctuations around 0.1 Hz (the reciprocal of 10 s). Importantly, the correlation time series during naturalistic movie segments were aligned to the beginning of the stimuli, for each run.

*2.2.5. CNN architecture and feature extraction*

As a representative model of the visual hierarchy, we employed AlexNet, a Convolutional Neural Network (CNN) trained on object classification using a dataset of millions of natural images (ImageNet). This CNN model is composed of five convolutional layers and three fully connected layers. Each layer of the CNN extracts different features from an image. As in visual cortical areas, convolutional layers are composed of many neurons, each one selective to a small region of the space resembling the receptive field of real neurons, grouped in channels selective to different features (i.e., different orientations). Higher convolutional layers also have bigger receptive fields in channels selective to increasingly complex features, such as object parts and shape. Finally, in fully-connected layers each neuron responds to the whole image, as in higher-order visual regions. For the aim of this study, from the eight layers of the CNN, layers 1, 2, 6 and 7 were used to extract features to each frame of the movie. Specifically layers 1 and 2 extract low-level image features (edges, luminance) and layers 6 and 7 extract high-level image features (object recognition, semantics). Layer 1 was composed of 96 channels with 56x56 neurons each, layer 2 had 256 channels with 27x27 neurons each while layer 6 and 7 had 4096 neurons each. We employed the pretrained AlexNet from MATLAB's (MathWorks Inc.) deep learning toolbox.

In order to compare the BLP signal and the CNN output, every signal extracted from CNN was aligned with the beginning of the BLP signal. Also, the two time-series were trunked at the shortest length, across the subjects. Then, CNN output was subsampled at a frequency

of 5Hz by averaging the samples in 200ms windows. All analyses were performed on MATLAB 2016b, running on Ubuntu 18.04.3 LTS.

*2.2.6. Dimensionality reduction*

For each convolutive layer (layers 1, 2) we reduced the dimensionality of the 3D matrix by averaging the CNN response to a specific filter across the NxN dimensions. As a result, we obtained a 1x1xfilter vector (e.g., for layer 1 a volume of 55x55x96 signals is reduced to 1x1x96). This average procedure was repeated for each time point (200 ms). Because the output of the fully connected layers (layers 6, 7) was already in the form of 1x1xUnits, this step of the analysis was not required. As a result, the data size was timeXoutput (where output was filter or unit). This size varied depending on the specific layer (e.g., layer 1: 1214 X 96; layer 2: 1214 X 256 layers 6-7: 1214 X4096).

To reduce the computation burden and also to remove the redundant information, we performed a Principal Components Analysis (PCA). To identify those components explaining the greatest variability across the responses of the filters or units, we performed PCA separately for each layer. After standardization, we applied spatial PCA to each layer, decomposing it into the product of layer PCs (matrix dimensions 1214 ×PC) and the related weights (PC × Output). The number of PCs to be kept for the next analysis was determined by applying a threshold of 95% to the cumulative percentage variance explained by the PCs.

*2.2.7. Multivariate Linear Decoder*

We used a linear decoder to map the CNN output to BLP functional connectivity. Each BLP-connectivity time course was treated as the target of the linear regression. Particularly, a stepwise analysis was applied to directly compare the amount of contribution of each feature while ensuring that the amount of variance explained is not being overfit.

To take account of possible delays between the artificial response (CNN output) and the biological response (BLP connectivity), the stepwise procedure was calculated by shifting the BLP correlation with a step of 200ms up to a maximum of 38s (Betti et al., 2013). Thus, for each pair of nodes, we obtained a "synthetic response" which reflects the linear combination of artificial response weighed to the regression coefficients. The responses derived from layers 1 and 2 represent the

processing of low-level features while layers 6 and 7 reflect the processing of high-level movie features.

*2.2.8. Lagged Pearson Correlation: BLP-DNN*

To quantify the relationship between the BLP functional connectivity and the synthetic response during the movie observation, for each layer and separately for each band we applied a lagged correlation by using the Pearson Coefficient. This consists of calculating the Pearson Correlation Coefficient (PCC) between BLP connectivity and the synthetic response with the same shift of stepwise calculation for the entire duration of two responses. By considering a 200ms step and the maximum delay of 38 sec, we obtained 191 lags.

The output of this analysis is a correlation value for each pair of nodes and for each lag. Because in our analysis we are interested only in the positive relationship between the biological and the synthetic response, we only considered in-phase relationships. Negative correlative values were set to NaN. Because the aim of the study was to characterize the variation of the biological response depending on low-level features (e.g., contrast, luminance, edge) or high-level features (e.g., object recognition, semantics) of the image, we quantified the Power Spectrum Density (PSD) to ensure that the spectral content was not significantly different across layer 1 and 2, and layer 6 and 7. To do so, we applied a periodogram method with rectangular window length equal to the signal (N=1214). The PSD was computed independently for each column of the PC's matrix and the spectra were averaged in order to obtain a single PSD for each layer. A paired t-test was performed to evaluate significant differences in the spectral content of the signals in the frequency range [0.01-0.5 Hz] ($p=0.01$ corrected for multiple comparisons with Bonferroni correction). Because the outputs of layers 1-2 and layers 6-7 were not significantly different, the lagged correlation coefficients have been merged according to "OR" logic operator. This analysis step was performed to take into account possible NaN values. In this way, for each band, we obtained a correlation matrix between the BLP connectivity and the movie low-level features and a matrix between the BLP connectivity and the movie high-level features. From now on, we refer to them as level features. These analyses were repeated for each subject.

*2.2.9 Time lag statistical test*

For each subject and band, correlation coefficients were transformed using the Z-Fisher transformation. Each z-score value was standardized (that is, it is divided by the standard deviation of the distribution (1/N-3), with N number of time-points. These values were then averaged across subjects. Once obtained the z-scores group-level matrices for each band and level feature, we applied a statistical threshold. To obtain this threshold, we estimate 100 surrogate signals for each node pair. These surrogate signals were obtained by randomly shuffling the correlation values between node-pairs, while preserving their position in a given lag. For each node pair, we estimated the mean and the standard deviation, and then we defined the corresponding threshold as the mean + 1 standard deviation. The correlation values below the threshold were discarded for further analysis.

The correlation values above the threshold were assessed by one-tailed statistical z-test. A Holm correction was applied to account for multiple comparisons, yielding an estimate of significance ($p<0.05$, corrected for the number of node pairs to be tested in each lag). Values that were not statistically significant are discarded (set to NaN values). In addition, to ensure the robustness of the results over time, z-values that are not significant in at least two consecutive lags are rejected. At the end, we obtained matrices of nodes-pair*lag size (120x191).

To determine whether the association between the biological and the artificial response occurs at a specific temporal window, we estimated the Probability Density Function (pdf). For each group-level matrix, the distribution of the correlation values was fitted with a Kernel function, separately for each band and level feature.

*2.2.10. ANOVA*

Before running an ANOVA design, we applied specific analysis steps to the single-subjects correlation matrices. For each subject, band, and level feature, the matrices were thresholded using the same approach used for the group-level matrices. The correlation values above the threshold were assessed by a statistical test. Each value was converted to a normal distribution using Fisher Z-Transformation and tested with a one-tailed z-test. A Holm correction was then applied as for the group-level matrices.

To test significant differences between bands and level features, we performed a two-way ANOVA (band: 2 levels and level feature: 2 levels) analysis. The pdf curve was used as a guide to study the response delays for each subject, selecting the time range in which the pdf has values greater than 10% of its maximum. Specifically, for every pair of nodes, we computed the center of gravity of the response delay (lag), and then for each subject, we obtained a 16x16 matrix ( 10 nodes in the Visual network, and 6 in the Dorsal) in each band and level feature. For each subject, we selected the lag values (excluding the diagonal and considering the upper part of the matrix) and calculated the response delay.

## 2.3. Results

Correlation coefficients were standardized across time and averaged across subjects. We first thresholded each node pair while preserving position in a given lag, then applied a one-tailed statistical z-test, and finally a Holm correction for the number of node pairs in each lag. To determine whether the association between the biological and the artificial response occurs at a specific temporal window, we estimated the Power Density Function (pdf). For each group-level matrix, the distribution of the significant correlation values was fitted with a Kernel function, separately for each band and level feature.

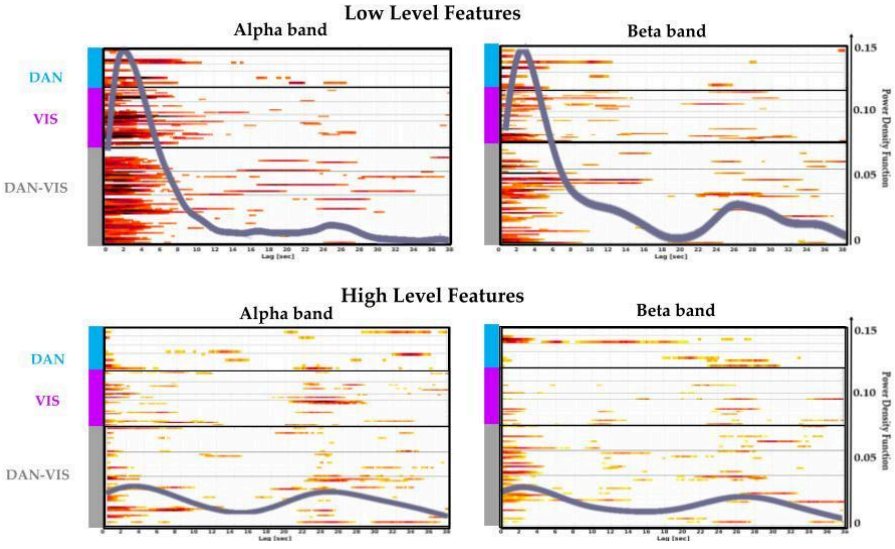

**Figure 2.2 Mean power density spectrums** representing the significant connectivity coefficient correlations between MEG BLP and DNN in different level features and bands over time between and within networks . The X-axes represent 191 lags (200ms steps of 38s lags) and the y-axes the nodes (VIS, DAN, and VIS-DAN). The distributions characterize the functional connectivity over time in different bands processing different level features.

Results show a clear sparse distribution over time in high level features as opposed to low level features for both bands. The difference between alpha and beta is highlighted in the low level features: low-level processing can affect the BLP functional connectivity, well beyond the early stages of processing (10-16s and 24-32s) (Figure 2.2).

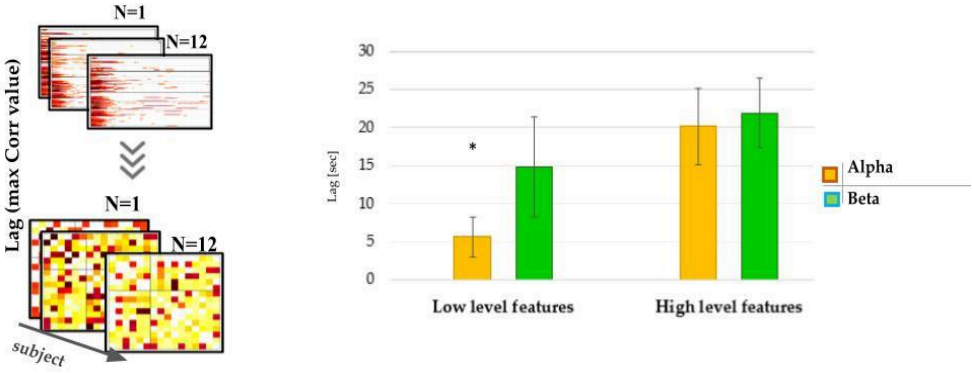


**Figure 2.3 ANOVA** On the left, a schematic of the thresholding of correlation coefficients at a single level subject. On the right, the 2x2 repeated measures ANOVA results. Low level processing in alpha is significantly different from all other distributions, and low level and high level feature processing is significantly different in time.

For the ANOVA (Figure 2.3), we selected one lag median per subject, level, band, and ROI and then considered both between (VIS_DAN) and within (VIS/DAN) connections. The 2x2 (level:low/high, band: alpha/beta) repeated measures ANOVA showed a significant main effect of level features (F(1,11)=32.57, $p$=.000), a significant main effect of band (F(1,11)=9.1812, $p$=.01), and a significant interaction (F(1,11)=16.842, $p$=.001). Post hoc Bonferroni analysis showed a significant difference for low level features between alpha ($M$= 6.485, $SD$= 4.058) and beta ($M$=14.85, $SD$= 6.6304) and a difference between alpha low level ($M$=6.485, $SD$= 4.0588) and alpha high level ($M$=20.167, $SD$=65.0547), and between beta low level($M$=14.85, $SD$= 6.6304) and beta high level($M$=22.01, $SD$=4.6418).

## 2.4. Discussion

*2.4.1. Lower level vs higher level features*

In the final experiment, we take advantage of the temporal power of MEG and a CNN, a representative model of the visual hierarchy trained on object classification. We aim to describe the biological variation over time of low level and high level features in the dorsal visual stream during visuospatial naturalistic viewing. We describe the dynamics of low level and high level features in alpha and beta frequency bands, the physiological RSN correlates (de Pasquale et al., 2010; Hacker et al., 2017) by correlating the output from the CNN to the MEG BLP data. Using a DNN model has been previously used to characterize the ventral visual pathway responsible for object classification, over very small temporal windows (first milliseconds). Here we, utilize the DNN to look at multidimensional and complex stimuli over windows of 38 seconds with a 200 ms lag in order to have a description of the subjective life experience, in accordance with the idea that integration windows can start with ms and go up to even minutes (Hasson, 2015). The main aim of the study was to characterize the time of the functional connectivity in lower level processing or higher level processing over naturalistic long delays in the dorsal visual pathway.

In accordance with the increasing TR (Hasson, 2015), our first results show a significant difference between low level functional connectivity time processing and high level. The functional connectivity processing of low level features has initial peaks, whereas in high level

processing, the function is sparse over time. Deep neural networks are modeled according to the hierarchical brain processing concept. This became a reliable tool particularly for the understanding of object processing in space, but also in time. For example, Cichy (2014) compared MEG signals of human object processing and DNN representations to describe the temporal processing in the ventral stream over the first hundreds of milliseconds. However such studies have described small integration windows that do not explain the subjective integration experience of everyday life. One of the inherent problems with experimental manipulation is the extreme control of the experiment in order to study only the desirable variables. However, we have an understanding of how the visual system reacts in a controlled environment: RFs decrease from lower level to associate higher areas, and similarly in time, TRws increase in a hierarchical manner. For example, we have known for a long time that the earliest integration windows are as small as 150 ms for motion integration (Gibbon et al., 1997) and 300 ms for apparent motion (Kolers, 1972), but processing semantic integration windows can go up to minutes (Hasson, 2015) where if two pieces of information fall in the same integration window then they will be understood as one. The functional modulation of low level feature processing over long naturalistic windows has been mainly studied in the speech literature with storytelling. For example, Hasson and colleagues (2015) studied both the visual (silent movie) and auditory system (7 minute story-telling) to characterize TRWs over different integration windows. In the visual domain, the longest integration windows have been proposed to be up to 3 seconds after which the perceptual load of the naturalistic videos becomes too much to integrate ideas. Fairhall and colleagues (2014) find that low level features do not affect the perceptual integration window and propose two mechanisms at play: a fast lower level processing to account for visual change and the higher level integration process window that takes up to 3 seconds. These two processes are very important since natural viewing requires a constant integration of information or continuous integration of prior information as opposed to working memory, that is the retention of information with active maintenance. As opposed to Fairhall and colleagues (2014), we find that the earliest peak of activity is around 6 seconds for lower level features. This does not oppose the existence of two mechanisms, one of faster integration and another separate process at a later interval. However, here we emphasize the importance of studying and defining even longer

naturalistic windows allowing us to confirm particular peaks of integration for lower level features, as opposed to sparse coding of higher level features.

Sparse coding is a concept that has been applied mainly to space; here we also show the mechanism in time. Each awake moment we have massive inputs of visual data and our brain needs to process all this information in an efficient way to understand what is relevant. Even if we do not know exactly (or still understanding) how cortical circuits manage this, we have general principles that explain it. One such principle, sparse coding, was proposed first by Barlow (1972): the brain should reformat this sensory data maintaining full representation with the smallest possible number of neurons. It does so by adapting to the statistics of the inputs allowing neurons to become selective to particularly recurring patterns (Olshausen & Rozell, 2017). The reason this principle has great appeal is because it lends an explanation to learning and creating associations or bridging in higher order areas, by still explicitly maintaining the structure and features of the images, all while reducing energy.

Our results can also be relayed to the difference between shifting attention and maintaining attention, two mechanisms that are at play in the dorsal attention network at very short time intervals (Spadone et al., 2021). Whereas lower level processing requires the immediate shifts of attention and therefore faster processing, higher level features that need to be maintained show a sparse curve of activity. Our results extend the literature and suggest the existence of such mechanisms even at longer temporal processing times.

In summary we confirm the existence of functional temporal windows that are a lot longer than those described in the literature to assess for the first time the temporal activity of functional connectivity processing of lower level features vs higher level features. We find that whereas lower level features are processed at certain peaks (6 seconds in alpha and a later 15 second peak in beta), higher level features are processed in non-precise sparse intervals.

*2.4.2 Alpha vs Beta*

Our results show a significant interaction between bands and level features. Alpha and beta fluctuations are the main correlates of resting state connectivity. Compared to rest, alpha BLP connectivity decreases both in natural scene videos and scrambled videos both

within and between networks, whereas beta BLP connectivity decreases only for scrambled videos and not natural movie clips. Centrality dynamics and spatial distributions were similar in movie clips and at rest in beta but not alpha (Betti et al., 2018). This suggests that beta rhythm integration is similar at rest and during natural vision. A possible explanation is that beta band reflects task related intrinsic activity, reflecting visual or semantic information (Betti et al., 2018). Our results then can be explained by a system where beta might mediate top-down priors, that facilitate the bottom-up communication of attended stimuli (Lee et al., 2013; Bastos et al., 2015), whereas alpha might mediate top-down influences suppressing irrelevant background (Van Kerkoerle et al., 2014) creating priors to be processed bottom-up. This separate role of alpha and beta is further pronounced in visuospatial experiments. When attention is shifted to the right hemifield, alpha decreases in the contralateral left hemisphere and increases in the ipsilateral right hemisphere (Sauseng et al., 2005). This effect has been noted on a single trial basis across different modalities. When the receptive fields in V1 are exposed to different contrasts receiving inhibitory alpha, the higher contrasts will have a higher excitability drive and also overcome the inhibitory effect earlier in the cycle. This helps in segmenting the visual scene into a temporal code and explains why low level features are processed early on, and high level features show a late modulation. Instead, from language processing, syntactic binding or making lexical inferences cause an increase in beta coherence whereas action verb production creates a decrease in beta power (Weiss & Mueller, 2012), and beta enhancements are important for integration over seconds, and understanding natural visual events has the same timescale (Betti et al., 2021). Findings show that beta is stabilizing the percept or reflecting its accuracy (Donner et al., 2007; Kloosterman et al., 2015). For example, Donner and colleagues (2007) found that beta in the dorsal visual pathway is predicting the accuracy rather than the content of the perceptual reports of subjects, and suggested that beta is indexing, and potentially controlling, the efficiency of the neural computations behind perceptual decisions. Similarly, Kloosterman and colleagues (2015) show that beta amplitude is reflecting the perceptual change of the bimodal moving stimuli, and Piantoni and colleagues (2010) show that synchronized beta activity amplitude is reflecting the size of active neural coalitions, where less likely percepts are associated with smaller coalitions. This body of literature reasons that beta triggers a top down mechanism modulating

the amplitude and allowing the stabilization of the newly selected perceptual interpretation and reflects a status quo role that is maintained also at later lags. Our characterization of low level and high level features processed in alpha and beta over long interval windows confirm that beta and alpha have different functional roles supported in animal (Michalareas et al.,2016) and human studies (Bastos et al., 2015) investigating neural synchrony. However, we extend the literature to describe different temporal behaviors in low level vs high level features: Whereas alpha and beta processing times for high level features are sparse and show the same behavior, beta and alpha are involved in the processing of low level features at earlier intervals, however, beta peaks also at a later interval. Even if beta and alpha can be phase-locked if they arise from the same neural generator, they can also be separate. Our results reflect a similar mechanism, where alpha and beta behave differently in lower level processing, but show a similar temporal behavior or sparse curve in higher level processing.

*2.4.3. Dorsal pathway*

Function of the dorsal attention system can be described from action observation studies. In the action observation literature, ventral and dorsal networks are at play. The ventral network explains the features with ever more complexity, while the dorsal attention nodes relay visual to motor representation, and are involved in constant feedback with the sensorimotor system to anticipate next movements. Infact, the activity in the sensorimotor system is activated during observation and execution. The areas involved in this mirror-like behavior are the precentral gyrus, inferior frontal, and inferior parietal area/intra sulcus. According to Wolpert and Ghahramani (2000), mirror-like activity is possible through both the forward and inverse models. The hypothesis is that inverse signals from predictive fronto-parietal areas are merged with forward information to understand others' intention after simulation. Sebastiani and colleagues (2014) suggest that the neural correlates of those are along the beta and alpha phases. Infact, in the sensorimotor area mainly, mirror-like activity (observation/execution) is usually described with the u rhythm, that is a mix of both alpha (8-12) to beta (20-25). The u rhythm arises from the harmonic beta (20) and alpha (10) mixture. Whereas in execution alpha, beta, and u are all found to be the same, in observation there is a posterior-anterior sequence in alpha and a simultaneous fronto-parietal activity in beta. This suggests that beta has a predictive

role, since it is involved in status quo and motor activity, it could be assessing the precision of the expected sequence of movements, to increase the efficiency of feedback.

As such the function of the dorsal pathway has been studied in the visual stream along very quick timescales abundantly, however, few studies investigate information accumulation and the function of the ventral and dorsal stream in long temporal naturalistic windows. Our aim was to characterize the difference in functionality in the dorsal visual brain over long intervals, where millisecond signaling cannot be accounted for anymore. Language studies map temporal windows for word, sentence, and paragraph processing along the VAN and DAN that go up to 38 seconds (Lerner et al., 2011). One study aimed to map the temporal windows along the dorsal visual stream (VIS and DAN) (Shi et al., 2017). They compare fMRI data of subjects watching short clips of movies with a trained RNN (Recurrent neural network). RNNs integrate spatial and temporal information, providing a hierarchical and distributed model of visual processing memory. Unlike CNNs, RNNs learn spatiotemporal features from videos, enabling better action recognition and predicting cortical responses to natural movie stimuli, particularly in dorsal stream visual areas. They map windows up to 8 seconds, and find a significant difference in temporal windows in the early visual area and in the higher dorsal attention nodes. Given the evidence of the function of DAN along longer timescales, here we map this change in different bands at different level features.

*2.4.4. Limitations*

One limitation of the study is that MEG and CNN data had to be heavily preprocessed in order to reduce complexity. This downsampling may possibly be removing important temporal and spatial information. However it is important to note that our MEG data was used in earlier studies and already preprocessed. Moreover, to take account of possible delays between the CNN output and the biological response (BLP connectivity), a stepwise procedure was calculated by shifting the BLP correlation with a step of 200ms up to a maximum of 38s as proposed by Betti et al., 2013. Moreover, the already selected nodes are based on prior fMRI studies that yield reliable resting-state network (RSN) classification at the individual subject level even if limited in the prefrontal and tempopariaetal regions (Hacker et al., 2013). We acknowledge that our choice of nodes affects all subsequent analyses, but we chose to have a consistent pipeline with the previous

studies using this MEG data (Betti et al., 2013; Betti et al., 2018). On that note, the next step would be to replicate these results using different parcellations, and exploring more networks.

# Chapter 3

## The representation of hands in the resting somatomotor area

### 3.1. Introduction

The hand is an active sensory organ. Daily, we rely on its physical and motor properties to grasp and manipulate objects, often under visual guidance. This ability also depends on proprioception and touch. These two sensory systems track the movement of the hand and convey information about the objects respectively. Therefore, visual and haptic information co-occur (Ernst & Banks, 2002) with the motor counterparts, especially during everyday manual behavior. Sensory afferents and movements are represented in the primary somatosensory (S1) and motor cortices (M1) (Penfield and Boldrey, 1937; Merzenich et al., 1978; Rizzolatti & Luppino, 2001; Schieber, 2001). Notably, however, recent studies in healthy individuals showed non-afferent processing of visual stimuli within the primary somatosensory cortex (Kuehn et al., 2018). It is unknown, however, whether such multisensory response maps reflect the co-occurrence statistics occurring during natural manual behavior. Having "access" to the visual and sensorimotor properties of the hand can be an efficient strategy for the brain to interact with the features of everyday objects rapidly. Recent studies show that information from the visual to the motor cortex has a short latency, and that the connection is facilitated during visuomotor stimuli, possibly contributing to visuomotor integration (Strigaro et al., 2015). The perception of static body stimuli suggestive of fluent movement recruits the motor area shown by an increase in oxygen dependent responses in M1 and SMA and an increased functional connectivity between the two areas (Orgs et al., 2016).

Recent theoretical and empirical studies (Betti et al., 2021; Pezzulo et al., 2021; Livne et al., 2022) suggest that statistical regularities of the body and environment may be coded in resting brain activity. The spontaneous activity observed when the participant lies quietly at rest, without any sensory input nor motor output (Fox & Raichle, 2007), may have a role in encoding such multisensory representation of the

hand more than other biological stimuli. Previous electrophysiological and neuroimaging studies show that, rather than being random noise, the spontaneous activity is highly structured in space and time, as observed by (for a review (Deco & Corbetta, 2011; Raichle, 2011)). However, there is still no consensus on its functional role and computations.

The first systematic investigation addressing the spatiotemporal structure of the spontaneous activity focused on the hand region of the primary somatomotor cortex. Through interregional correlations at rest, or resting-state functional connectivity, authors found that the topography of the somatomotor areas is similar to that evoked by finger movements (Biswal et al., 1995). One possible interpretation of Biswal's (1995) findings could be that the internal representations of the hand at rest resemble those during touch and action (Wang et al., 2013). This begs whether the resting (somatomotor) brain retains traces of everyday experience with the hand, either visual, motor, or somatosensory. If this hypothesis holds, it can suggest that the internal hand model is stable, present even at rest, and multisensorial, encompassing the visual and somatomotor aspects. Stimulus-evoked patterns are linked to spontaneous multi-voxel activity patterns, mainly in the stimulus's preferred brain region (Kim et al., 2020). Furthermore, the cortex processes coincidentally occurring information (Blake et al., 2002). These two aspects support the interpretation that the co-occurrence of vision and usage of the hand are represented in the generic patterns of the resting somatomotor cortex.

Building on this evidence, we hypothesized that the multivariate patterns of BOLD resting-state activity in the somatomotor cortex retain a high similarity with patterns of the multivariate task-evoked activity elicited by visual hand stimuli. If the internal model adapts to natural stimuli (Berkes et al., 2011), this effect should be specific for natural hands but not for hand-shaped objects (such as robot hands or gloves) or control stimuli (*i.e.,* food). Given that intrinsic representations are specific for the stimuli being coded in that area (Kim et al., 2020), we expect this effect in the hand but not the foot area of the somatomotor cortex. Finally, we also do not expect this effect in the early visual areas that code low to mid-level features. We calculated rest/task coherence using both the kolmogorov-smirnov test and the U90 cutoff (Kim et al., 2020). As opposed to the kolmogorov-smirnov test, the U90 cutoff captures the frames of resting state over time with

the highest coherence with the average multivoxel activity of a category. While the kolmogorov-smirnov test evaluates the whole of two distributions to determine a goodness of fit, the U90 cutoff correlates multivoxel task-related patterns with those extracted from each time point of the resting-state to generate cumulative distribution functions using the upper 90th percentile as a measure of strength of coherence between stimulus group and rest patterns for each ROI and subject. This allows us to highlight the differences in the tails of the distributions. Both our kolmogorov-smirnov and u90 results confirmed that an internal representation of the static hand, not suggestive of any motion, is coded in the left somatomotor region. Specifically, this representation was lateralized to the left, in hand, but not the foot area. This representation was found in the early somatomotor areas but not in the visual cortex, suggesting that it might be used for its inferred use. This is further confirmed by the trend analysis showing that the *internal* hand representation is stronger than that of the robot hand or glove.

## 3.2. Materials and Methods

*3.2.1. Subjects*

Twenty healthy individuals (10 females) were enrolled in the study (mean age ± SD 29 ± 2.59, range 24-34). All subjects underwent medical interviews and examinations to rule out the history or presence of any disorders that could affect brain function and development. Participants were provided with a detailed description of all the experimental procedures and were required to sign a written informed consent. The study was conducted under a protocol approved by the local ethical committee (protocol n. 1485/2017) according to the Declaration of Helsinki (Association, 2013). All subjects were right-handed, following the Edinburgh Handedness Inventory. We discarded one subject from subsequent analyses because of excessive movement artifacts in fMRI data, leading to a final sample of nineteen subjects.

*3.2.2. Design and Stimuli*

The paradigm was divided into three parts. The first part included an eight-minute resting-state scan (pre-task scan). During the resting-state scan, subjects fixated a red cross (24 x 24 degrees) at the center of the screen (VisuaStimDigital dual-display goggles, 32 x 24 degrees of visual angles, Resonance Technology Inc.), without

performing any cognitive or motor tasks. In the second part, we presented subjects with pictures of four categories of objects , natural hands, robot hands and control stimuli (i.e., food). All stimuli had the same vertical orientation. Left and right hands presented from the front and from the back were randomly selected and presented. We used six different examples for each object category. We presented subjects with five four-minute runs: in each run, subjects attended twelve randomized blocks (three categories, four blocks each). Each block lasted 12 seconds, followed by 8 seconds of fixation, and included 20 randomized repetitions of the six category stimuli, each presented for 0.3 seconds and followed by fixation for 0.3 seconds. Participants were instructed to perform a covert working memory one-back task as in the first task. Each run began and ended with 20 seconds of rest to acquire baseline fMRI activity. For the stimulus set, we used pictures of items pertaining to the four categories, which were converted to grayscale and matched for global luminance and root-mean-squared (RMS) contrast to control for low-level visual biases. The object pictures were centered and embedded in a circular pink-noise display with a fixed circumference (16 degrees) blending into a gray background.

For the third part, subjects performed a three-minute finger tapping localizer scan. We instructed them to tap their thumb on every other finger of their right-dominant hand sequentially and at their own pace (blocks of 15 seconds of activity followed by 15 seconds of rest).

All the visual stimuli were presented using MR-compatible display goggles (VisuaStimDigital, Resonance Technology Inc.) covering 32 x 24 degrees of visual angle, and a PC running MATLAB (MathWorks Inc, Natick, MA, USA) and the Psychophysics Toolbox version 3 (Kleiner et al., 2007).

*3.3.3. MRI Data Acquisition*

We used a Philips 3T Ingenia scanner with a 32-channel phased-array coil. We used a gradient recall echo-planar (GRE-EPI) sequence with TR/TE = 2,000/30ms, FA = 75°, FOV = 256 mm, acquisition matrix = 84 × 82, reconstruction matrix = 128 × 128, acquisition voxel size = 3 × 3 × 3 mm, reconstruction voxel size = 2 × 2 × 3 mm, 38 interleaved axial slices, and 240 volumes. We also acquired three-dimensional high-resolution anatomical images of the brain using a magnetization prepared rapid gradient echo sequence (MPRAGE) with TR/TE = 7/3.2ms, FA = 9°, FOV = 224 mm, acquisition matrix =

224 × 224, acquisition and reconstruction voxel size = 1 × 1 × 1 mm, 156 sagittal slices.

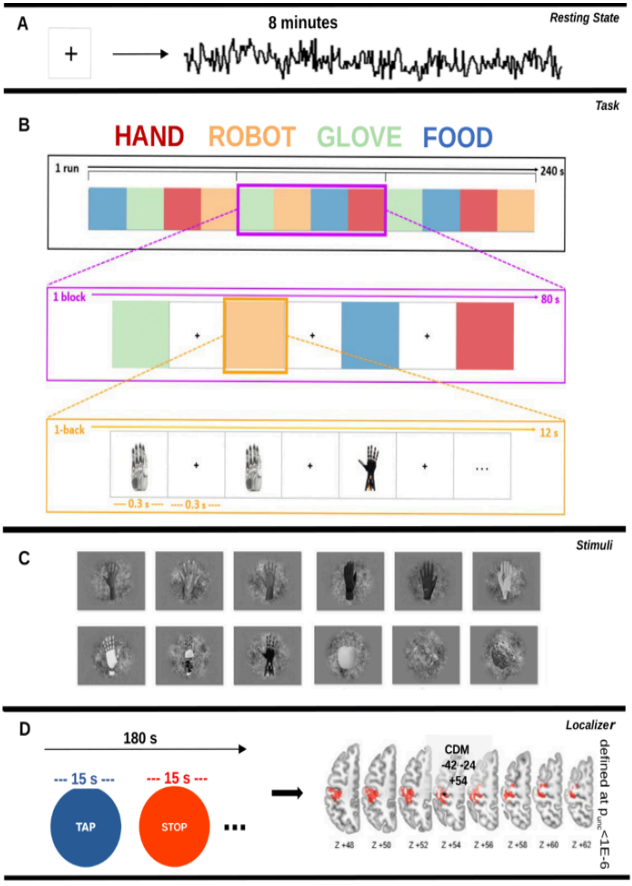


**Figure 3.1 Experimental design and visual stimuli** The experiment consisted of 3 phases: i) pre-task resting-state scan (A), ii) 1-back rapid block design with four categories (B), and iii) finger tapping localizer scan (D). Visual stimuli are represented in (C).

*3.2.4. Preprocessing*

We used the AFNI software package (Cox, 1996) and a standard preprocessing pipeline to preprocess fMRI data, separately for tasks (i.e., visual working memory and finger tapping) and resting-state runs. We temporally aligned the runs (3dTshift), then corrected for head motion (3dvolreg), and used the transformation matrices to compute the framewise displacement, identifying time points affected by excessive motion (Power et al., 2012). We then spatially smoothed the data using a Gaussian kernel and an iterative procedure up to 6 mm Full Width at Half Maximum (3dBlurToFWHM). We then normalized the runs by dividing the intensity of each voxel over its mean over the time series and applied a multiple regression analysis (3dDeconvolve) to estimate the activation patterns for each category. We aimed to show that the hands' category would be more strongly represented in resting state somatomotor hand-preferred areas. For each subject, we modeled a GLM that included the four stimulus categories (hand, robot, glove, food) for the visual working memory task and the finger movement blocks for the hand motor localizer. The output was a stimulus-evoked BOLD multi-voxel task (category) beta weight. We included head movement parameters, framewise displacement, and signal trends as nuisance variables. We performed a generalized least squares time series fit for the resting-state data to account for nuisance regressors defined above and signal autocorrelation using an autoregressive moving average model (order 1). We registered single subject results and preprocessed rest scans to MNI152 standard space (Fonov et al., 2009) using nonlinear registration.

*3.2.5. ROIs*

We selected three regions of interest (ROIs) to test the association between resting-state spontaneous activity and task-evoked activity. We identified the left somatomotor area after thresholding ($p<10^{-6}$ uncorrected) the finger tapping localizer, resulting in a small ROI (~5,000 µL) encompassing the precentral and postcentral gyri, as also suggested by the overlap with the HCP atlas (Glasser et al., 2016). The center of gravity of our ROI is -42 -24 54 (MNI atlas) and is only 6.34 mm far apart from the hand knob considering the classical paper of Chouinard and colleagues (Chouinard and Paus, 2006) (-38 -28 52) and 8.75 mm considering Yoshimura and colleagues (2017) (−34±4, −25±3, 57±11). Then, we selected the right somatomotor area by left/right flipping the ROI mentioned above (3dLRflip). We defined the bilateral

early visual cortex (V1, V2, V3) using VisFAtlas (Rosenke et al., 2020) as a further early sensory control region. .

*3.2.6. Multi-voxel pattern analysis*

In the main analysis, we first analyzed the association between resting-state and each task-evoked multivoxel activity using a 2-sample kolmogorov-smirnov test. We performed for each ROI a rANOVA with 4 levels of task/rest coherence according to the four stimulus categories. In order to characterize our dataset better, we calculated the empirical cumulative distribution function (ECDF) that represents the tails of the distributions of task/rest coherence. Given that task specificity was represented with distributions with heavy-tails, we also used the U90 cutoff introduced by Kim and colleagues (Kim et al., 2020) (Figure 2). For each category group, we computed a cumulative distribution function that represents the strength (r2) of the correlation between the average multivoxel category representation and the patterns from every time point of the spontaneous activity. Briefly, the patterns of task-evoked activity of the four stimulus categories (hand, robot, glove, food) were extracted in each subject and ROI. We correlated (using 1-pdist2, 'correlation' distance on MATLAB) the z-scored multivoxel activity of task conditions and with the patterns of all resting state timepoints. This procedure ultimately generated a distribution of correlation coefficients for each stimulus category, ROI, and subject (Figure 2). As in (Kim et al., 2020), we saved the u90 measure (90th percentile) pattern association for each task condition to measure task/rest congruence. This approach, recently adopted by other studies (Livne et al., 2022; Kim et al., 2020; Zhang et al., 2023) constitutes a representative measure of the relationship between patterns of resting state activity and those evoked by a category (averaged task-evoked vectors). The U90 value is a transparent estimation of spatial similarity since it refers to the value of a correlation coefficient suggesting the degree of similarity between task-evoked and resting-state activity patterns. This cut-off has a statistical rationale: values below could be closer to the mean of the distribution (mean=0), while values above 90th percentile could be a few, and not representative of the population. In order to compare our data to Kim and colleagues (2020), we additionally inspected the skewness (calculated as mean of pattern association - median of pattern association / standard deviation) and the spread (calculated as the variance of the pattern association) of the data. In the main analysis, we performed for each ROI a rANOVA,

modeling the u90 values across 4 levels (according to the four stimulus categories) and applied Sidak corrections post-hoc.

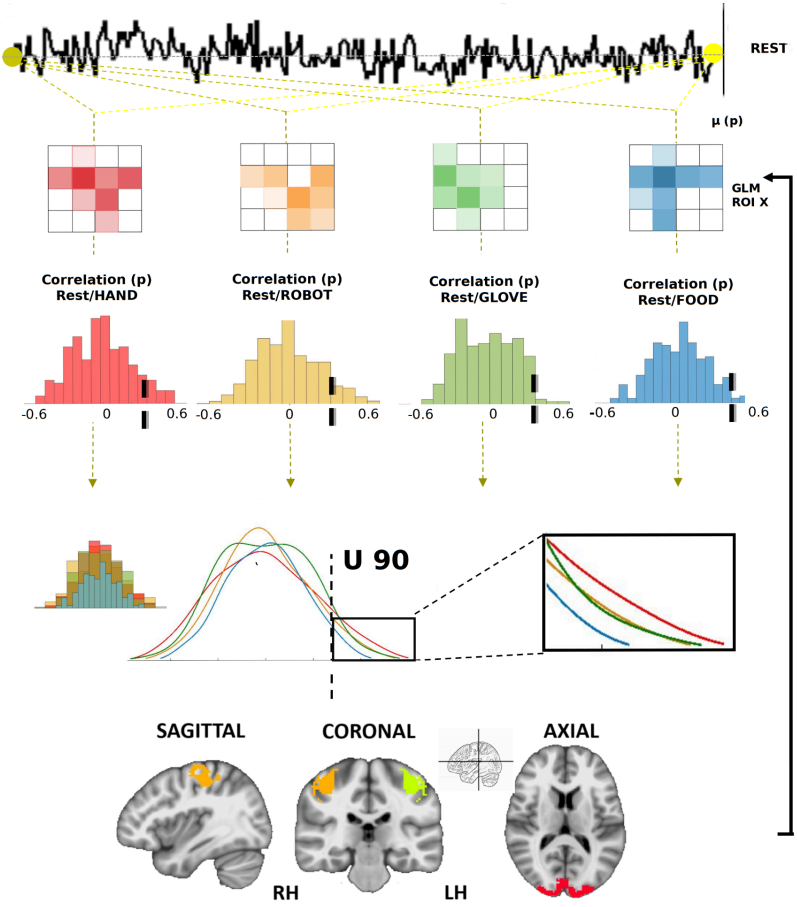


**Figure 3.2 U90 analysis** We extracted the activity patterns elicited by the four stimulus categories in each subject and ROI and correlated them with those extracted from each time point of the resting state. We considered the upper 90% (U90) from the distribution of correlation coefficients for each stimulus category, ROI, and subject to measure task/rest congruency for the ANOVA. Each subject then had 4 U90 measures.

Further follow-up analyses in the left somatomotor ROI included a trend analysis to test *a priori* hypotheses of differences among stimulus categories (hand>robot>glove>food), an analysis suited for exploring post hoc ANOVA interactions. Finally, we performed a searchlight analysis (radius=6 mm) in a larger extent of the left somatomotor cortex ($p<0.0001$, uncorrected) to better highlight the subregions of the postcentral and precentral gyri involved in the association between task and rest activity.

## 3.3. Results

In this study, we examined whether the human somatomotor cortex codes at rest for a visual representation of the hand and its inferred use. Using functional magnetic resonance imaging (fMRI), we acquired an eight-minute resting-state scan in which observers kept their eyes on a fixation point without any explicit cognitive or motor task (Figure 3.1A). We then presented observers with pictures of four categories of stimuli, *i.e.,* natural hands, robot hands, gloves, and control stimuli (*i.e.,* food) (Figure 3.1B-C). We were interested in testing two main predictions. First, we predicted that the somatomotor cortex would represent at rest more commonly hand vs. non-hand stimuli. This is given by the nearly continuous vision of our hands in everyday life, compared to hand-like stimuli like robot hands or gloves. These stimuli share visual attributes with hands but are much less common. Second, inferred action/use may also modulate spontaneous activity in the somatomotor cortex. Robot hands perform similar action to hands, while gloves have no autonomous motor attributes, despite their relative visual similarity. To test the association between resting-state spontaneous activity and task-evoked responses, we selected three separate regions of interest (ROIs): left and right somatomotor areas (*i.e.*, precentral and postcentral gyri), identified with a three-minute finger tapping scan (Figure 3.1D), and bilateral early visual areas (V1-V2-V3) selected using a functional atlas of the visual cortex. For further specificity, we then selected the foot somatomotor area, by creating a sphere with 7.5 mm radius around the center of gravity coordinates (+4, −30, 68) to make sure that our effect is specific to the hand specialized somatomotor area.

For each ROI we extracted both task-evoked and rest multivoxel activity and calculated the coherence using a Kolmogorov-smirnov test. To highlight the differences characterized

with distributions with heavy tails, we then compared the mean multivoxel activity of each stimulus object to the patterns of every time point of resting state. This resulted in 4 vectors (for 4 stimulus groups) of Pearson's r values representing the strength between the stimulus and rest patterns and can be represented with 4 cumulative distribution functions(CDF). We compared the CDFs considering only the upper 90th percentile as a cutoff.

We performed a 1-way rANOVA comparing the kolmogorov-smirnov correlation values for each rest/category group across subjects in each region of interest (left, right somatomotor, bilateral visual) and then used the same approach for the U90 values. Using the kolmogorov-smirnov test, the 1-way rANOVA yielded significant differences (after Bonferroni corrected threshold) between rest/category group correlations in the left somatomotor ROI (Figure 3A), ($F(3,54)=4.194$, $p=.009$, $\eta 2=18.90$), but not in the right somatomotor ROI (Figure 3.3 C) ($F(3,54)=0.84$, $p=.47$, $\eta 2=4.50$) or in the early visual areas (Figure 3.3 E) ($F(3,54)=1.13$, $p=.34$, $\eta 2=5.92$). Using the U90 values, we confirm the significant results after Bonferroni correction only in the left somatomotor cortex, where the hand stimuli yielded the strongest rest-task similarity as compared to non-hand stimuli or objects (Figure 3.3 B) ($F(F(3,54)=4.825$, $p=.005$, $\eta 2=21.14$). Posthoc comparisons using Sidak correction ($p<0.05$) indicate that the hand condition ($M=0.283$, $SD=0.017$) is significantly higher than the food condition ($M=0.232$, $SD=0.011$). Instead, in the right somatomotor area, the 1-way rANOVA using U90 correlation values showed no significant main effect of conditions ($F_{(3,54)}=.641$, $p=.592$, $\eta 2=3.44$), confirming that the effect was left-lateralized (Figure 3.4 B). Finally, as expected, there were no differences in correlation in the non-hand-preferred early visual areas (Figure 3.4 C) that extract low- to mid-level visual features controlled for in our stimuli (Burkhalter and Essen, 1986; Hubel and Livingstone, 1987) where the 1-way rANOVA showed no significant main effect of conditions ($F_{(3,54)}=1.423$, $p=.246$, $\eta=.073$).

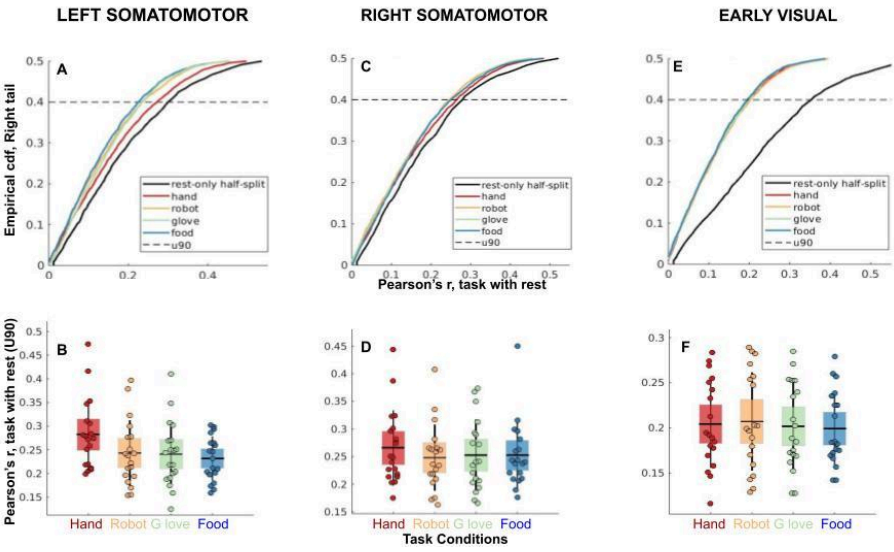


**Figure 3.3 ECDF and U90 (A -C -E)** As visualized with the ECDF representing coherence between rest and task category (hand/robot/glove/food) in the left somatomotor **(A)**, right somatomotor **( C)**, and early visual areas **(E)**, main differences were found in the positive tails of the distributions. For visualization purposes, we added the ECDF of the resting state pattern alone, and the u90 equivalent cutoff. **(B-D-F)** We further used the approach of (Kim et al., 2020) who used the upper 90% cutoff (U90) of the distribution of correlation values to measure task-rest multi-voxel pattern similarity. We show separate rANOVAs in the left somatomotor **(B)**, right somatomotor **(D)** and early visual areas **(F)**: The x-axis shows the 4 categories, and the y-axis shows the U90 correlation of task-rest. Each dot represents a subject. In the right somatomotor hand region (B) and early visual areas (C), the rANOVA showed no significant main effect of conditions ($p<0.05$). Instead in the left somatomotor area the rANOVA shows a significant main effect of visual categories ($F(3,54)=3.469$, $p=.022$, $ETA=.162$).

In the left somatosensory area, we followed up with a trend analysis for exploring post hoc the rANOVA interactions and testing the differences among stimulus categories (hand>robot>glove>food) (Figure 3.4). Here, the aim is to better understand the multimodal activity highlighted by the visually induced effect. This investigation revealed a significant trend for decreased task-rest similarity in the multivoxel spatial pattern going from natural hand to hand-shaped objects (e.g., glove) ($F(1,18)=9.055$, $p=.008$, $\eta=.335$) (Figure 3.4 B). Finally, a searchlight analysis (radius=6 mm) in a larger extent of the left somatomotor cortex ($p<0.0001$, uncorrected) was performed to better highlight the subregion of the postcentral and precentral gyri involved in the association between task and rest activity. Interestingly, this region falls in the post-central gyrus in correspondence with the hand notch (Figure 3.4 C). or in the somatomotor foot area ($F_{(3,72)}=0.25$, $p=.862$, $\eta=.96$).

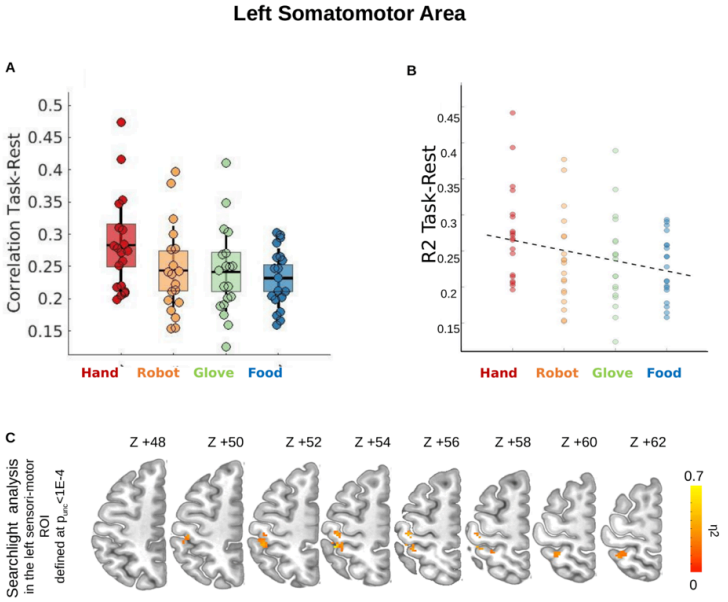


**Figure 3.4 Results in the left somatomotor area** (A) ANOVA: The x-axis shows the four categories, and the y-axis shows the U90 correlation of task-rest. Each dot represents a subject. The ANOVA

shows a significant main effect of visual categories (F(3,54)=3.469, p=.022, ETA=.162). (B) the graph shows a significant linear trend (hand>robot>glove>food) (F(1,18)=9.055, p=.008, ETA=.335). The x-axis shows the 4 categories, and the y-axis shows the R2 of the task-rest correlation. Each dot represents a subject. (C) The lower part shows a searchlight analysis shows the task-rest association critically depends on the postcentral gyrus activity.

## 3.4. Discussion

Hands are regularly in sight in everyday life. This visibility affects motor control, perception, and attention, as visual information is integrated into an internal model of somatomotor control. Spontaneous brain activity, *i.e.,* ongoing activity in the absence of an active task (rest), is correlated among somatomotor regions that are jointly activated during motor tasks. Moreover, recent studies suggest that spontaneous activity patterns do not only replay at rest task activation patterns but also maintain a model of the statistical regularities (priors) of the body and environment, which may be used to predict upcoming behavior. Here we test whether spontaneous activity in the human somatomotor cortex is modulated by visual stimuli that display hands vs. non-hand stimuli and by the use/action they represent. We analyzed activity with fMRI and multivariate pattern analysis to examine the similarity between spontaneous (rest) activity patterns and task-evoked patterns to the presentation of natural hands, robot hands, gloves, or control stimuli (food). In the left somatomotor cortex, we observed a stronger (multi-voxel) spatial correlation between resting-state activity and natural hand picture patterns compared to other stimuli. A trend analysis showed that task-rest pattern similarity was influenced by inferred visual and motor attributes (i.e., correlation for hand>robot>glove>food). We did not observe any task-rest similarity in the visual cortex or the foot specialized somatomotor area. We conclude that somatomotor brain regions code at rest for visual representations of hand stimuli and their inferred use.

### *3.4.1. Encoding of the hand form in the resting somatomotor regions*

In the case of hand, use and visibility often co-occur, with beneficial effects on behavioral performance: hand visibility improves the accuracy of volitional movements (Desmurget et al., 1997), reduces the perception of pain (Longo et al., 2009), increases the tactile perception (Kennett et al., 2001), and allows motor-visual regularities

that compute the sense of agency (Wen & Haggard, 2020). During the interaction with the external objects, we also rely on an intrinsic model of body structure to mediate a sense of position (Longo & Haggard, 2010; Longo et al., 2010). Other evidence suggests that the brain employs a standard posture or a Bayesian prior for guiding body-space perception and action (Romano et al., 2021). This is interesting in light of the idea that spontaneous activity maintains statistical regularities (priors) to anticipate and even predict environmental demands (Raichle, 2011). This hypothesis has been tested using natural visual stimuli and common cognitive tasks (Betti et al., 2013, 2018; Spadone et al., 2015; Kim et al., 2020; Livne et al., 2022). More specifically, the idea is that during offline periods, the brain forms generic priors or low-dimensional representations, as categories or synergies, rather than individual instances or movements, that summarize the relative abundance of visual stimuli, objects, or motor patterns in the natural environment. Interestingly, this reduced subspace of summary representations is formed along a hierarchy that has the somatomotor cortices at the lower level (Pezzulo et al., 2021). Consistently, our results show that at rest the hand somatomotor region maintains a multivoxel pattern of activity that resembles that evoked by the presentation of the natural hands compared to control stimuli (e.g., food). We use two methods to correlate our data: While the Kolmogorov-Smirnov test evaluates the whole of two distributions to determine a goodness of fit, the U90 cutoff correlates multivoxel task-related patterns with those extracted from each time point of the resting-state to generate cumulative distribution functions using the upper 90th percentile as a measure of strength of coherence between stimulus group and rest patterns for each ROI and subject. This allows us to highlight the differences in the tails of the distributions. Therefore, the somatomotor regions acting as a central node of processing of afferent and efferent inputs, fundamental for the active tactile feedback and proprioception, may retain low-dimensional representations (e.g., the body form) during the offline periods, instrumental to the interaction with the environment. We often rely on the physical properties of our body (especially the hand) to grasp and manipulate objects and the co-occurrence of sight and use contribute to generate priors tied to the actual experience. According to the idea that things occurring nearly coincidentally in time are represented together in the cortex (Blake et al., 2002), i.e., cutaneous, proprioceptive, and visual signals, the co-occurrence statistics of usage and visibility may be represented in the

somatomotor regions. Despite diverse spatial and temporal resolutions, previous findings in humans have demonstrated the existence of preferred tuning of single neurons to visually cued non-grasp-related hand shapes in the posterior parietal cortex (Klaes et al., 2015). Moreover, in monkeys, a substantial number of neurons in the arm/hand region of the postcentral gyrus is activated by both somatosensory and visual stimulation (Iriki et al., 1996). Here, for the first time, we found that the rest-task similarity in the somatomotor cortex is driven by the hand form, and we can access it through a visually cued paradigm without explicit motor processing.

Our results align with the multimodal role of M1/S1 that embodies different body/motor-related representations, including the one mediated by hands. Linguistic studies show correlates of action words in the somatotopic activation of the motor and premotor cortex (e.g., Hauk et al., 2004; Raposo et al., 2009). Similarly, embodied cognition theories suggest that understanding action verbs is reliant on the involvement of action-related areas; this representation is found to be body-specific. For example, right- and left-handers perform actions differently and use different brain regions for semantic representation (Willems et al., 2009).

In summary, the stability of the spontaneous activity suggests that this set of neural signals is a possible candidate to preserve long-term models and priors of common behaviors and natural stimuli (Betti et al., 2021; Pezzulo et al., 2021). These prior representations are the result of statistical learning mechanisms that store the co-occurrence statistics of hand visibility and usage, instrumental to the exploration and manipulation of the surroundings.

*3.4.2. An interplay of visual and motor attributes modulates the match between resting and task-related activity.*

From birth, humans learn to use their hands in a more refined and precise fashion to interact with external objects. Spontaneous activity has been hypothesized to reflect recapitulation of previous experiences or expectations of highly probable sensory events. More precisely, the ongoing activity could be related to the statistics of habitual cortical activations during real life, both in humans (Betti et al., 2018; Strappini et al., 2018; Kim et al., 2020) and animals (Yao et al., 2007; Berkes et al., 2011). For example, in (Livne et al., 2022) a higher similarity between motor and spontaneous patterns have been shown

for natural hand sequences than for novel sequences. Based on these findings, our results can be interpreted as evidence that rest-task similarity reflects natural stimuli, or more specifically, hand-like objects as compared to artificial ones. More recent studies have found that this effect is higher in stimuli-selective regions (Kim et al., 2020).

Beyond being natural, hands have sensory and motor attributes. From a visual point of view, gloves and robotic hands share with the hands both size and shape, but they are non-living items with either synthetic motor properties such as the robot, or no independent motor attributes such as the glove. While the visual attributes may explain the similarity between rest and task activity induced by the natural hand compared to control objects (i.e., food) (Figure 3.3 A/C), the inferred action/used can bias such similarities along a continuum where hands are higher, as tied to natural movements, than robotic hands performing similarly, yet unnatural, and gloves, without autonomous motor attributes (Figure 3.4 B). The interplay of these factors offers an interpretation of the rankings obtained: on top of the continuum, the natural hand, most abundant environmentally, has necessary visual features and motor attributes, then the robot hand though not as environmentally abundant, has the same visual features and synthetic motor attributes, the glove retains only the visual features but cannot act on its own, and finally the food objects neither have the same visual nor motor attributes.

Studies in the visual cortex demonstrated that the long-term natural experience shapes the response profile. The high-level cortical representations of these regions capture the statistics with which visual stimuli occur (Simoncelli & Olshausen, 2001; Chan et al., 2010). Furthermore, animal studies demonstrated that when visual stimuli are natural scenes, the reliability of visual neurons' response increases and persists in the subsequent spontaneous activity; these effects are not observed with the stimulation with the noise of flashed bar stimuli (Yao et al., 2007). In the ferret's visual cortex, the tuning function of neurons "learns" the statistics of natural but not artificial stimuli as the animal grows (Berkes et al., 2011). Here, for the first time, we found evidence of visual representations encoded in non-visual regions at rest, but regions still specific to our hand stimuli (hand notch area). Thus, we believe that the cumulative impact of the statistics with which natural stimuli occur during the development and the experience shape the ongoing activity of the whole brain, not limited to the visual cortex. Our results are

confirmed and opposed by Stringer and coworkers (Stringer et al., 2019) that show representations of natural motor sequences at rest in the mouse visual brain but also across the forebrain. Similar to our results, they confirm that natural sequences are coded in resting state and shape the activity of the whole brain, but conversely, they find motor sequence representations in the visual system. The discrepancy could be explained by the fact that our stimuli did not represent any actions (i.e., strictly open hands), and the fact that spontaneous activity in mice is recorded differently than in humans (mouse running in darkness vs humans staring at a cross with eyes open). However, their results similarly show evidence of generic multimodal representations encompassing both motor and visual attributes.

Our results could be alternatively interpreted as a result of motor imagery. Very early works have found that motor imagery (i.e., imagining a movement without executing it) has been found to share overlapping networks with motor performance (Porro et al., 1996). However, we can exclude the possibility that our participants were engaged in hand motor imagery during the resting state scan, since that was acquired before the presentation of the visual stimuli task and they were naive to the aim of the study.

*3.4.3. The representation of the hand in the somatomotor area is left-lateralized*

Our study shows that the multi-voxel activity of hands in the somatomotor area is most represented in resting-state activity; this effect was lateralized to the left, not the right, somatomotor area (Figure 3.4 B). From a theoretical point of view, the lateralization result is well aligned with the existing literature: compared to other body parts and objects, static pictures of hands and tools have overlapping activations in the LOTC that are then selectively connected to the left intraparietal sulcus and left premotor cortex (Bracci et al., 2010; Bracci & Peelen, 2013; Lingnau & Downing, 2015). Moreover, a body of literature shows bilateral motor cortical activations are produced with the left non-dominant hand. In contrast, movements with the dominant right hand induce only contralateral (left) activations (Rushworth et al., 2001). Precisely, visuospatial orientation attention, measured with eye movements, activates a network of premotor and parietal areas in the right hemisphere, while motor attention and selection, measured as the attention needed to redirect a hand movement, activate the left hemisphere (Schluter et al., 1998; Kuhtz-Buschbeck et al., 2003). TMS and lesion studies further support this left lateralization, describing

motor selection, motor attention, or motor learning (Schluter et al., 1998; Rushworth et al., 2001). The effector independent activation in the left hemisphere is also found in kinesthetic motor imagery that activates common circuits for motion in the premotor, posterior parietal, and cerebellar regions (Kuhtz-Buschbeck et al., 2003). More recently, Karolis and colleagues (Karolis et al., 2019), using fMRI, built a lateralization functional taxonomy along four axes representing symbolic communication, perception/action, emotion, and decision-making. Along the action/perception axis, the categories movement, finger tapping, motor observation, and touch were all found to activate the sensorimotor areas of the left hemisphere selectively. Interestingly, all these categories had the term hand or finger as the principal components with the highest loadings.

In summary, we provide the first evidence that the ongoing activity in the left somatomotor regions maintains a long-term representation of the hand shape in the absence of any motor task or sensory stimulation. Furthermore, this result may lend support to the representation of visually related information in M1/S1 enforcing a multimodal role in these areas.

*3.4.4. Limitations*

The most significant limitation of our study is the use of highly controlled still images. Stimuli presented were in black and white with noise imposed on top to correct for low and mid-level features. This is necessary as a first step since we are looking for generic representations in resting state activity and are using early visual regions as a control. Since resting state patterns represent the statistical regularities of the environment, as a next step, more naturalistic stimuli (for example, videos) should be used as opposed to our non-naturalistic images.

On a methodological note, our ROIs encompass both the pre and post-central gyrus; even though the searchlight analysis shows the task-rest association critically depends on the postcentral gyrus activity, giving more spatial specificity to the effect, further studies should entangle the hand region alone. Moreover, since kinesthetic motor imagery activates the left premotor, posterior parietal, and cerebellar regions and is effector-independent (Kuhtz-Buschbeck, 2003), this would help us rule out mental imagery as a possible explanation of our results.

*3.4.5. Conclusion*

The sensory and perceptual analysis is not only dependent on external stimuli but also on the coding of expected features in the surroundings simultaneous to the flow of information (Engel et al., 2001). Building models of the environment create generic priors that are stable and common across individuals yet malleable with experience and age (Betti et al., 2021). If motor-sensory interactions are entrained throughout development into spontaneous cortical oscillations, then our internal model must have a reservoir of natural behaviors. Our experiment shows that spontaneous activity representing the internal model, despite its apparently noisy structure, reliably encodes the visuospatial topography of the natural human hand in somatomotor areas. This suggests that the human hand represents a prior for the effective motor interaction with the external environment to allow exploration, learning, and adaptation. In line with the malleability of the cerebral cortex in response to behavior and other input manipulations, to our knowledge, this is the first experiment to show that visually-conveyed representation of hands in resting-state activity in frontoparietal somatomotor areas by looking at the relationship between evoked and spontaneous activity. By measuring coherence between evoked activity and resting state activity, we shed light on a multimodal role of the somatomotor areas.

*3.4.6 Significant Statement*

The functional role of spontaneous brain activity still needs to be defined. Existing literature suggests the resting human brain preserves representations of the statistical regularities of the body and the environment. The hand is the primary means to build regularities, used to interact with the surroundings. Using fMRI, we test the hypothesis that the spontaneous activity in the human somatomotor cortex is modulated by visual stimuli that display hands vs. non-hand stimuli and by the use/action they represent. Results show a strong spatial correlation between resting-state activity and hand pictures in the left somatomotor cortex compared to the control conditions. Overall, the visual attributes of the human hand and its inferred use are already mapped in the resting somatomotor activity.

# Chapter 4

## The representation of observing common hand movements in spontaneous activity: movement at rest

### 4.1. Introduction

The interplay of the visual and motor system is essential for our survival; since we are toddlers, we learn from imitation and, as we grow older, understanding others' actions allows us to react in appropriate ways to navigate social situations. Learning and storing a repertoire of actions will allow us to navigate easier in our environment as we will have expectations of what will come up and how to react to it. It also allows us to identify irregularities or errors.

Action observation and execution are two mechanisms that recruit the same somatomotor, premotor, parietal and visual brain areas (Hari, 1998) allowing learning and encoding of actions. One of the biggest implications of these findings is that the sensorimotor areas can be rendered functional again after a trauma with only intense observation of the action (Iacoboni, 2001). The classic account explaining action understanding has typically been the simulation theory, where we compare the observed action by simulating it, activating a mirror neuron system. According to this account, familiar actions that are already in one's repertoire should evoke a higher activation in the action observation network (AON). Alternatively, there exists an inferential process that does not assume the existence of mirror neurons. According to the predictive theory account, an unexpected or erroneous action should evoke a higher activation since there is a mismatch and a bigger prediction error. The simulation account is supported by literature that shows that the AON is more activated when observing familiar actions (Buccino et al., 2004; Calvo-Merino et al., 2005; Shimada et al., 2010). This is because the action observation system codes for biological movement, for example artificial hands evoke less activation than real hand actions in premotor areas (Tai , 2004) and the AON is not activated for observed biomechanically impossible movements in the motor and parietal areas (Stevens et al., 2000). Interestingly, observing errors in actions of another human hand

interfered with the parallel execution of that action, while watching a robot hand doing an error did not interfere with the simultaneous execution of the action (Kilner et al., 2009). However, literature describing the response of the action observation network (AON) to human error mostly reports an increase in BOLD activation to error versus common activity (Hardwick, 2018; Monfardini, 2013) supporting the predictive coding account.

Given the mixed results, another way to understand the mechanisms of AON evoked activity, could be to compare it to resting state data. Naturalistic stimuli in seconds, minutes, or hours allow the study of adaptive brain functions; a common set of networks allows the separate processing of streams of information and the integration of relevant information for further cognition or behavior. Given these distinct yet cooperating brain networks, a large literature compares naturalistic paradigms to resting state with the aim of substituting it for the study of brain architecture in patients or children (Sonkusare, 2018). This would allow the increase of power by removing noise such as uncontrollable loss of vigilance , boredom, sleepiness, and motion in resting state. Resting state literature suggests that the brain at rest preserves representations of the statistical regularities of the body and the natural environment (Livne, 2020; Pezzulo et al., 2021; Betti et al., 2021). Abundant work shows similarities between task-driven and resting state intrinsic driven activity (Berkes et al., 2011; Strapini et al., 2019; Kim et al., 2020). When comparing external evoked activity with a spontaneous internal process, recent findings suggest a higher similarity between resting state spatial multivoxel patterns and patterns elicited by common hand movements as opposed to uncommon (Livne, 2020). Here we use the same method to study the coherence between resting state spatial multivoxel patterns and the patterns evoked by observing common and uncommon movements. We expect that resting state patterns will be more coherent with patterns of observing common movement.

However it has also been demonstrated that low frequency fluctuations persist in cognitive and behavioral tasks. Task-evoked functional connectivity is a mixture of spontaneous signals and stimulus- evoked signals; stimulus-evoked FC is not the only contributor to FC difference between task and rest scans(Lynch, 2018). In the second part, we filter stimulus evoked high frequencies and compare low frequency fluctuations (LFFs) in the different conditions

(common vs uncommon) and correlate them to resting state LFFs. According to the predictive theory account, functional connectivity of uncommon activity should be higher than common due to a bigger mismatch and prediction error, and the functional connectivity of common movements should be more correlated to resting state data that codes regularities. We therefore expect that 1) visual task related modulations of LFF FC will be more pronounced when observing non-naturalistic actions, 2) watching motor execution performed in a common/naturalistic way as opposed to uncommon, has a more similar LFFs FC architecture to that of resting state.

## 4.2. Methods

*4.2.1. Behavioral Stimuli*

In order to develop our stimuli, we recruited eighteen healthy subjects (8 females) , all right handed according to the Edinburgh Handedness Inventory and asked them through a series of both open-ended and forced-choice instructions to lift a cup in one of two scenarios; three cups inserted equidistantly (left center and right) or two cups (left and right). The instructions started open-ended (lift a cup) and then increasingly forced. This was done to come up with a scale that describes the most common to the most uncommon hand lifting gestures. The variables collected included left or right hand, position of the cup, and type of grasp. We asked the subjects to pick up the cups without defining a final aim. We manipulated our variables in open and forced conditions depending on distance, effector (left or right), and type of grasp, to map the probability of using different compositions to grab a cup. We found that regardless of position, right handed subjects (as scored on the Edinburgh Handedness Inventory) in a free scenario, use their right whole hand 100% of the time. Subjects were only likely to choose a pinch if forced to choose between that and an arm and twist rotation. This is because we made sure our cups do not have any handles or anything suggestive of using a pinch (3rd principle component synergy, Ingram et al., 2008). Interestingly, we found that subjects were equally likely to pick up the cup in the right position with an uncommon (twist of the arm) right whole hand, and a common (straight extension/flexion) left whole hand. This could be mediated by the varied final aim of picking up the cup. Given that the aim modulates the type of behavior and brain activation (Koch et al., 2010), we made sure that all our subsequent fMRI videos clearly show the aim

of picking up the cup (placing it on a shelf). Given that pinch grasp and whole hand grasp both activate M1 equally, even if they produce different muscle activations (Koch et al., 2010), we grouped them together in either the common (straight arm) or uncommon (twisted arm) groups.

*4.2.2. fMRI Participants*

We enrolled twenty nine healthy individuals (18 females) in the study (mean age ± SD 28.34 ± 1.34, range 23-38). All subjects underwent medical interviews and examinations to rule out the history or presence of any disorders that could affect brain function and development. Participants were provided with a detailed description of all the experimental procedures, were required to sign a written informed consent, and received compensation. The study was conducted under a protocol approved by the local ethical committee (protocol n.2016/679) according to the Declaration of Helsinki (2013). All subjects were right-handed, following the Edinburgh Handedness Inventory. We discarded three subjects from subsequent analyses because of excessive movement artifacts in fMRI resting state data, leading to a final sample of 26 subjects.

*4.2.3. fMRI design and stimuli*

The design was made up of three main parts. We first collected 15 minutes of resting state data. We asked subjects to maintain their view on a fixation cross (24 x 24 degrees) in the middle of the screen and not to think about anything in particular. The second part was the main task. We presented subjects with 3 second videos in two main categories (common and uncommon behaviors) that were defined after the behavioral experiment. Both categories included 12 sub-categories with variations in hand (left or right), cup position (left, center, or right), and hand posture (whole hand and fine grasp). Videos had female and male hands and 7 cup colors that were randomly selected for presentation. All videos were taken in the same room with equal luminance and a green background, from a first person point of view. We presented all 24 sub-categories in each run. Videos were presented in a block design, where twosubgroups (subblocks) of each category were presented in alternation (CC-UU.. or UU-CC), each made up of 5 videos (3 seconds each) presented out of the 14 (given female/male and cup color variation) available samples for that subgroup. Each of the 3 runs lasted for 9 minutes. We asked subjects to maintain their focus on

the videos presented. The final part was a finger tapping block design task. We asked subjects to tap their index on every other finger according to their own pace and randomized blocks of left and right hand, and rest for 15 seconds each. Subjects followed the instructions on the screen that told them whether to use the left or right hand or to rest. Each block was repeated 4 times.

*4.2.4. fMRI Data Acquisition*

We used a Siemens Magnetom Prisma 3T scanner (Erlangen, Germany) with *a* 32-channel head coil. We used a multiband T2* weighted EPI sequence with a slice acceleration factor of 4, no in-plane acceleration, TR/TE = 1100/30ms, FA = 65°, FOV = 208x208 mm2, acquisition and reconstruction matrix = 86 x 86, voxel size = 2.43 mm3, 60 axial slices. All EPI scans included 4 dummy scans. Fieldmapping was performed with the blipup/blipdown method, by acquiring two spin-echo EPI volumes with phase encoding in opposite direction, no multiband acceleration and the same geometrical and sampling properties of functional runs (TE = 80 ms, TR = 7000 ms). We also acquired three-dimensional high-resolution anatomical images of the brain using a magnetization prepared rapid gradient echo sequence (MPRAGE) incorporating perspective motion correction and selective reacquisition of data corrupted by motion based on interleaved 3D EPI navigators (Tisdall et al., 2012) with TR/TI/TE = 2500/1100/2ms, FA = 8°, FOV = 256x240 mm2, acquisition matrix = 256x240, acquisition and reconstruction voxel size = 1 × 1 × 1 mm3, 176 slices per slab.

*4.2.5. Preprocessing*

We used the SPM8 software package (2014) and a standard preprocessing pipeline to preprocess fMRI data separately for each task (visual working memory, finger tapping, passive visual viewing of videos) and the resting state data. We first discarded the first 3 dummy scans of every run. To account for B0 distortions, fieldmaps were generated from the spin-echo EPI scans with opposite phase encoding polarity using the fsl topup tool (Holland et al., 2010). The Fieldmap toolbox was then used to convert fieldmaps to spm format. We outputted the VDM (voxel displacement matrix) and coregistered the field maps to the 1st EPI using the distortion corrected and averaged spin echo images as reference. Simultaneous distortion and motion correction, including motion x distortion interaction, was then applied (Andersson et al., 2001) then we applied a slice timing correction. We

then coregistered the T1 to the average EPI, normalized the T1-weighted scan using integrated normalization and segment (1mm) and applied the normalization to the EPI scans (2.4mm). Finally we smoothed the data with an isotropic Gaussian kernel (4.8 mm FWHM). For each subject, we fitted a GLM that included the two stimulus categories (common, uncommon) for the visual task and another for the finger movement blocks for the hand motor localizer with two categories (left, right). Additionally, for the resting state scans, we applied an ICA that takes into account motion confounds and derivatives. We registered single subject results and preprocessed rest scans to MNI152 standard space (Fonov et al., 2009) using nonlinear registration.

For further functional connectivity analyses, we used CONN toolbox (2020). The 3 conditions (rest - task1 - task2) were all treated similarly. We filtered the data from 0.01 to 0.12 and regressed out principal components of grey matter, white matter, CSF, motion, and the effect of the task. Removing the effect of the task is required before computing functional connectivity measures in task designs in order to remove the changes in BOLD signal directly associated with the presence or absence of a task and hence allows the comparison between resting state and task design data.

*4.2.6. ROI selection*

For the BOLD activation analysis, we identified the left and right somatomotor areas separately after thresholding for each subject alone the finger tapping localizer, resulting in 500 voxel ROIs, encompassing the precentral and postcentral gyri. We defined the bilateral early visual cortex (V1, V2, V3) using VisFAtlas (Rosenke et al., 2020) as a further early sensory control region.

For the functional connectivity analysis, we used the default CONN toolbox functional atlas divided into 8 networks and 32 ROIs, where for each ROI the average BOLD timeseries is extracted from the voxels.

*4.2.7. Multivoxel and statistical analysis*

The first aim of the study was to test whether there is a higher coherence between resting state BOLD activation and somatomotor BOLD changes related to viewing common activity as opposed to uncommon. For each subject and ROI we extracted the average multivoxel related activity to both common and uncommon categories

(3D t stats). We then correlated them to the pattern of every time point of resting state BOLD signal extracted from the same ROI (4D). This outputs for each subject and each ROI 2 r^2 vectors representing the coherence between the average multivoxel activity of the category and the timeframes of resting states. By considering the upper 90th percentile, we establish the strongest correlations between resting state frames and categories.For every ROI, we performed a 1-tailed paired-t test comparing the coherence measures for common and uncommon.

The second aim was to test the hypothesis that watching motor execution performed in a common/naturalistic way has LFFs with a similar FC architecture to that of resting state LFFs. Functional connectivity measures were calculated using the CONN toolbox with a whole brain parcellation with 32 ROIs and 496 connections. We calculated the weighted GLM ROI to ROI bivariate correlation functional connectivity measure using every ROI as a seed for every subject for the first level analysis. This outputs a 32x32 matrix for every subject for every condition (rest/common/uncommon). We first performed an all subjects between conditions paired-t test between common and uncommon categories in order to define and characterize the connections with significant increase or decrease in connectivity as a result of watching uncommon as opposed to common activity. Only connections with a significant increase or decrease (48 nodes) in connectivity were further considered. Then using Matlab, we computed the correlation measure between resting state and category LFFs using pdist function. This outputs two coherence measures (r values) per subject (between rest and each category). Finally, we performed a paired-t test between category coherence measures and obtained the p-value.

## 4.3. Results

In the right somatomotor area, we found a significantly higher coherence between resting state and multivoxel activity of common hand movements ($M$ = 0.033, $SD$ = 0.0744) as opposed to uncommon ($t(25)$ = 2.4, $p$ = .009) (Figure 4.1 A). The results align with our hypothesis showing common representation of motion at rest. In the left somatomotor area, we did not find any significant differences comparing coherence between resting state and multivoxel activity of viewing common hand movements ($M$ = 0.022, $SD$ = 0.0939) and uncommon ($t(25)$ = 1.4, $p$ = .08) (Figure 4.1 B). This shows that the

results were right lateralized. In the early visual areas, we found no significant differences comparing coherence between resting state and multivoxel activity of viewing common hand movements ($M$ = 0.002, $SD$ = 0.0302) and uncommon ($t(25)$ = 1.4, $p$ = - .24). As expected, there were no differences in correlation in the non-hand-preferred early visual areas (Figure4.1 C) that extract low- to mid-level visual features controlled for in our stimuli.

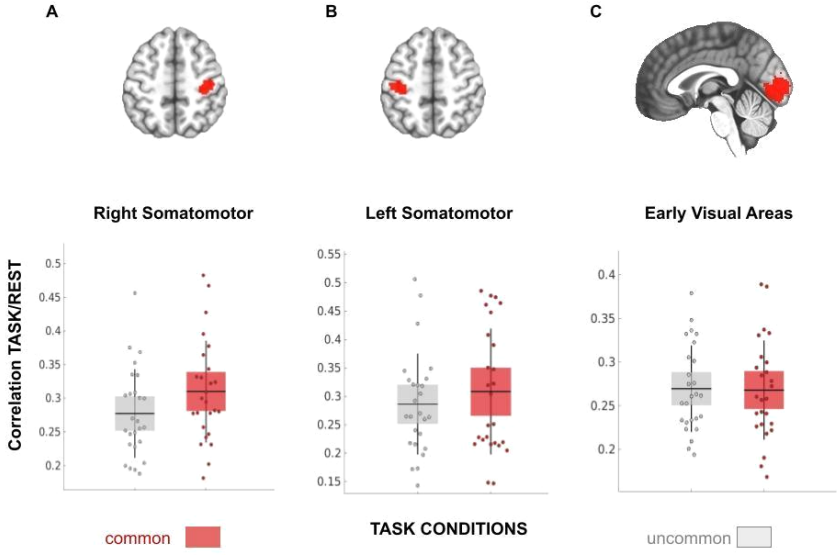


**Figure 4.1 Common-Uncommon grasp results** The upper panel shows example ROIs of the right and left somatomotor cortices and early visual areas. In the lower panel, the x-axis shows two categories (common/uncommon), and the y-axis shows the U90 correlation of task-rest. Each dot represents a subject. (A) The t-test shows that the visual category common is significantly higher than uncommon in the right somatomotor area (($t(25)$ = 2.4, $p$ = .009)), (B) no significant difference in the left somatomotor area ($t(25)$ = 1.4, $p$ = .08), and (C ) no significant difference in the early visual areas ($t(25)$ = 1.4, $p$ = - .24).

In the functional connectivity analysis, we used a whole brain parcellation to compute the connectivity measures for each category (rest/common/uncommon) for every subject. We then aimed to characterize the connections where LFFs significantly vary when watching common opposed to uncommon activity. We found significant differences in connectivity between common and uncommon conditions in 48 nodes ($p<0.05$) and a general increase of functional connectivity when watching uncommon vs common movements. Of interest, the biggest clusters with FC differences were between the visual system and the sensorimotor and dorsal attention networks. Finally, when comparing LFF FC of the two categories to rest, we found a higher correlation of FC between rest and common movement viewing as opposed to uncommon ($p=0.002$).

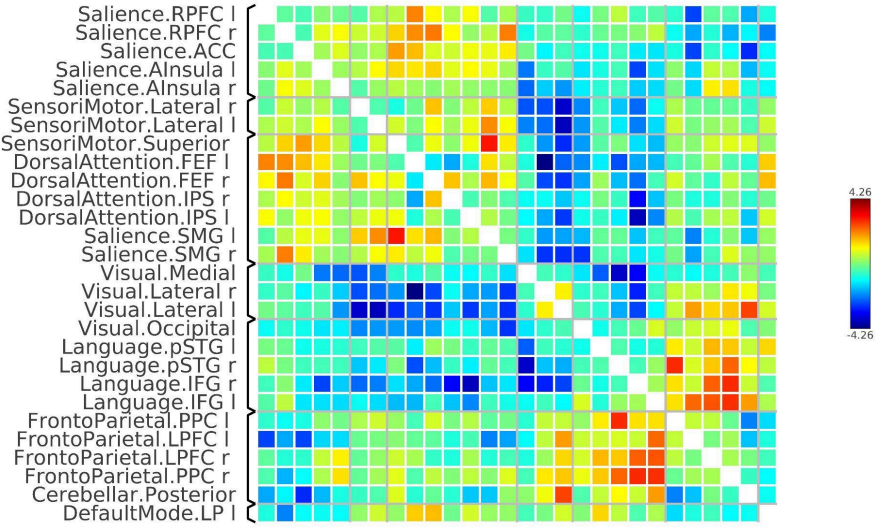


**Figure 4.2 LFF FC Common - LFF FC Uncommon** Red voxels signify an increase of functional connectivity when watching common vs uncommon movement, while blue voxels signify an increase of functional connectivity when watching uncommon vs common movements. We find significant differences in connectivity between

common and uncommon conditions in 48 nodes ($p<0.05$, uncorrected) and a general increase of functional connectivity when watching uncommon vs common movements (blue). Of interest, the biggest clusters with FC differences were between the visual system and the sensorimotor and dorsal attention networks

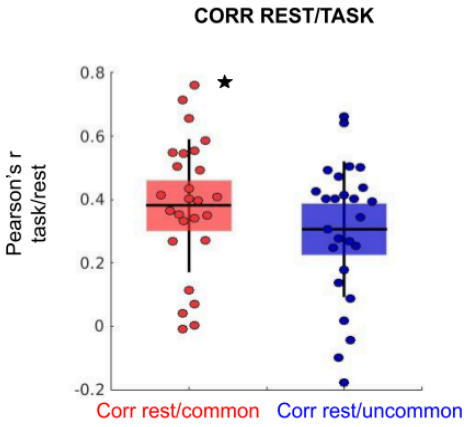


**Figure 4.3 Corr rest/task** The y-axis shows Pearson´s R values and the x-axis represents the two categories. Each dot represents a subject. We find a higher correlation of FC between rest and common movement viewing as opposed to uncommon ($p$=0.002).

## 4.4. Discussion

In this experiment, we hypothesize that activity of common action observation is retained in resting state spontaneous activity as opposed to activity of uncommon action observation. Three main conclusions can be drawn from our results. 1) The spatial multivoxel BOLD activity of the resting somatomotor area as it temporally fluctuates is more correlated with the multivoxel evoked-activity of observing common movements as opposed to uncommon. 2) Functional connectivity of low frequency fluctuations during externally

driven naturalistic stimulation reflects differences between watching common vs uncommon activity. 3) LFFs FC architecture of resting state is more similar to that of observing common activity as opposed to uncommon activity.

*4.4.1. Multivertex patterns of resting state and observing common hand movements are coherent in the right somatomotor area*

In the first analysis, we compared the rest and observation groups in the somatomotor area. For each category group, we computed a cumulative distribution function that represents the strength (r2) of the correlation between the average multivoxel category representation and the patterns from every time point of the spontaneous activity. The patterns of task-evoked activity of the two stimulus categories (common, uncommon) were extracted in each subject and ROI. We correlated the z-scored multivoxel activity of task conditions with the patterns of all resting state timepoints. This procedure ultimately generated a distribution of correlation coefficients for each stimulus category, ROI, and subject (Figure 4.2). As in (Kim et al., 2020), we saved the u90 measure ($90^{th}$ percentile) pattern association for each task condition to measure task/rest congruence. The U90 is a measure of coherence that captures the resting state multivertex spatial patterns of the temporally fluctuating signal that are most negatively or positively correlated with the multivertex GLM activity of the task. While the mean average values of correlations are 0 for all tasks, the tail captures the highest similarity values, i.e. spatial multivertex representation of resting state in windows most correlated with the multivertex representation of the task. Using this method, Zhang et al (2023) found that spatial resting state activity in the sensorimotor cortex is more coherent with common hand movements vs uncommon. Replicating this method, our results are aligned and extend the literature to show that the patterns of resting somatomotor area are also coherent with observing common hand movements.

Our general idea that action observation network related hubs can be detected in resting state networks is supported by the literature. For example, Molinari and colleagues (2013) used naturalistic videos of hand movements and compared ICA spatial maps of action observation of videos/static images and resting state networks in the same subjects. They found that the observation of natural hand actions can be reliably detected in healthy subjects with two ICA maps and that there is a big overlap of the parietofrontal network that can be identified in both

action observation and resting state. The parietal and frontal networks make up the core AON (Turella, 2013). Similarly, our results show that common action observation spatial maps are coherent with resting state patterns. We add to the literature by finding this effect in the extended AON, namely the somatomotor area.

*4.4.2. Widespread increase in LFF FC of observing uncommon hand movements vs common*

Our second results show a general increase of FC of low frequency fluctuations while observing uncommon hand movements as opposed to common. To our knowledge there is no fMRI work comparing spontaneous fluctuations filtered from externally evoked stimuli. Specifically, our observations indicate a general increase in low frequency activity in networks in frontal, parietal, sensorimotor, and visual areas for uncommon activity. Similarly, Errante (2019) found that the action observation network in naive participants was more activated watching naive participants prone to error perform novel complex actions but not to experts less prone to error, suggesting an increase in FC for erroneous or uncommon activity. Brass and colleagues (2007) found that an erroneous action in an implausible situation evoked a higher functional connectivity in the AON versus erroneous actions in somewhat plausible situations (opening a door with a leg if the hands are holding something). Given that all our videos had the same final aim of placing the cup on the counter, the most plausible common behavior is to use the first two main components that explain most variance of natural arm movement variance, flexion/extension in the sagittal plane and the modulation of the hand across the vertical plane (Averta, 2019).

However our results also show an increase mainly between prefrontal and IFG/SMG core AON nodes in FC activity for common movement. These results are also supported by the literature for example, Koch and colleagues (2010) found that while observing goal-directed movements induces corticocortical neurophysiological changes in the motor system, inappropriate grasping postures incongruent with the goal do not.

Our results then support both the predictive and imitation accounts: the predictive account expects an increase in LFF FC differences for observing uncommon activity, and the imitation account expects an increase in LFF FC of observing common movement.

Studying high frequencies, Gardner (2015) similarly found that the AON's connectivity with other brain regions can be dynamic. Specifically, the connectivity between the AON and the dorsolateral prefrontal cortex (DLPFC) increased during observation of familiar movements, whereas the connectivity between the AON and the posterior cingulate cortex (PCC) decreased during observation of familiar movements. These findings suggest that the brain's processing of observed actions is not static but rather dynamically modulated by the familiarity of the movements, and reflected even in lower frequency fluctuations.

*4.4.3. Resting state LFF FC is more coherent with LFF FC of observing common hand movements*

Finally, taking the functional connectivity map with significant nodes, we find that observing common hand movements is highly correlated with resting state LFF functional connectivity. Similar to our findings, Schurz and colleagues (2020) find overlap between action observation and resting state networks are highest in the DAN, VAN, and VIS. Zhang (2023) found that ecologically valid behavioral movements are more similar to resting state patterns in the SMN and DAN as opposed to unecological movements. We extend these results in the SMN and DAN to patterns of observing ecologically valid behaviors. However, as opposed to Zhang(2023), the VIS network was one of the main hubs. This is probably due to the nature of the different tasks of motion vs. observation.

Our LFF FC results taken together suggest that there is a bigger decrease of spontaneous activity in the uncommon as opposed to the common task. Brain activity during a task is a mixture of task-evoked activity and spontaneous activity or rather changes in emerging spontaneous networks (Lynch, 2018). According to this logic, during a task, spontaneous activity is suppressed. As a result, contrasting rest - task results in a decreased connectivity. This is expected because if spontaneous activity is decreasing then so is the intercorrelation. Therefore another explanation of our results could be that common, already learned, activity FC is more correlated with resting state FC because there is less spontaneous activity being suppressed than during the uncommon (unlearned) activity. In other words, observing common activity, an external activity, still retains internal resting state network correlations. Observing novel movements, however, further suppresses

internal correlations to allow the reconfiguration of networks for learning or attention processes.

*4.4.4. Limitations*

An inherent limitation of the u90 method is that it correlates multivoxel maps of activity with the patterns of every time point of resting state data, assuming independence of these data points. However, the u90 strength is its ability to capture the few windows in resting state with patterns most correlated to evoked patterns, instead of comparing evoked patterns to averages or fractions of resting state activity fluctuations over time. Another limitation pertains to our FC analysis. We had to start with a whole brain analysis to contrast LFF of common vs uncommon observation to assess where in the brain this difference is reflected in lower frequencies, to then do further analyses. Future studies should have a separate ROI scan. Notwithstanding the limitations, when taken together, both these analyses show that low frequency fluctuations retain statistical regularities in the natural environment and can dynamically change to accommodate the context.

# Chapter 5

# Discussion

## 5.1. Conclusions

By looking at FC changes of the VIS and DAN while watching naturalistic videos, we find that in a situation of continuous flow of information, low and high level features are processed at different intervals in different forms (chapter 2). The representation of low level features is abundant and imminent, while the representation of high level features is scarce and with seconds in delay (chapter 2). This scarce information could be stored in a generic form. For example, the multivoxel spatial representation of the observation of a hand, controlled for all low level features, is stored in the resting somatomotor area as opposed to the spatial representation of a food item (chapter 3). The somatomotor area is mainly active during movement and this is still represented in the low frequency fluctuations when it is at rest, here we show that so is the spatial representation of its form (chapter 3). The multimodal representation of the hand in scarce windows of resting state (u90) could facilitate the final aim of interacting with the environment. Moreover, the multivoxel spatial representation of observing common movement is more coherent with the resting somatomotor patterns than observing uncommon movement (chapter 4). Differences between the observation groups are detected in several networks in low frequency fluctuations (chapter 4). Given that stimulus evoked activity alone does not explain the difference between the internally driven and the externally driven brain, an externally driven brain has a mixture of spontaneous and evoked activity. By looking at differences in isolated low frequency fluctuations during external activity after removing the principal components related to the task, we shed light on how spontaneous activity is stable yet dynamically altered (chapter 4). We add to the literature that the connectivity architecture during the observation of common movement is more coherent with resting state low frequency fluctuations.

## 5.2. Naturalistic viewing and sparse coding

In this thesis, we consider both the visual system and the somatomotor region to study the representation of visual information during resting state. These two systems highly interact for effective manipulation of the environment. Several areas, including M1, are involved in reaching, and reaching to grasp, independent of object size and type of grasp (pinch grip- whole hand) (Di Bono et al., 2015). These areas are visually guided as shown by lesions to the area F1 (M1 equivalent in the macaque brain) that lead to the loss of control of individual fingers and coordination (Lawrence and Hopkins, 1976). Literature suggests that the anterior intraparietal sulcus could store the object's sensory properties (Murata et al., 2000). Animal studies show that visual information influences representations in area F5 (ventral premotor equivalent in macaque brain) and visual guidance in F2 (equivalent of dorsal premotor) (Raos et al. 2004). F5 chooses the most appropriate type of grip according to the visual information in AIP and sends the motor representations to F2 for visual guidance. F2 keeps memory of it for continuous update and reconfiguration as the hand approaches the object. The information is then sent to F1 for the final execution (Castiello and Begliomini, 2008). Similarly, V6A is in strong connection with the premotor cortex and like F2 elaborates space, motion, and visual representations to coordinate hand movement (Galetti et al., 2003; Gamberini et al., 2009). These two systems are also especially important during natural viewing that requires a constant integration of information and is part of a spatial and temporal hierarchy. Studying how the brain reacts to naturalistic stimuli and how the functional architecture is altered is important since the slow varying timescale of natural stimuli resembles that of spontaneous neural fluctuations (Hasson et al, 2008; Honey et al, 2012).

In the first experiment, we study the functional connectivity temporal architecture of naturalistic viewing in the visual dorsal system. The literature describes temporal receptive windows (TRWs) that increase as one moves from low level (sensory) to high level areas (perceptual and cognitive). For example, literature focusing on the posterior visual network has found that it integrates information over many seconds or minutes (Baldassano et al., 2017; Chen et al., 2016, Hasson et al., 2015; Simony et al., 2016). This temporal hierarchy has also been supported in the human auditory cortex (Sridharan et al., 2007; Stephens et al., 2013) and in non-human primate data (Chaudhuri

et al., 2015, Cirillo et al., 2018). The process includes a continuous integration of prior information as opposed to working memory, that is the retention of information with active maintenance. For the brain to adapt to the environment, it has to rely on dynamic interactions to achieve fast changes in the functional architecture of the brain. Temporal dynamics of neurons in different cortical areas can also be investigated by looking at the stability of their firing rate; looking at the decay time constant of the autocorrelation structure during a baseline period allows the computation of the neural intrinsic timescales (Ogawa and Komatsu, 2010; Murray et al., 2014; Cirillo et al., 2018). A similar approach has been used by others to investigate whether an ensemble of neurons within the same area, but with different functional classes, also had time scale differences (Nishida et al., 2014; Cavanagh et al., 2016; Fascianelli et al., 2017). All these studies have found that neurons with higher temporal stability maintained spatial information presented for longer and had slower intrinsic timescales. For example, FEF showed higher temporal stability than V4 (Ogawa and Komatsu,2010) and within the LIP, neurons specialized in maintaining information had slower intrinsic timescales (Nishida et al., 2014). This intrinsic time scale is useful for individuals in a dynamic environment: when fast changes are occuring, neurons with faster timescales are better suited and in more stable environments neurons with intrinsic slower timescales can be utilized. Results from the first experiment (Chapter 2) show that the functional connectivity of the brain during naturalistic viewing is also altered over longer intervals. Low level features show a peak at a window of 6 seconds. In the visual domain, the longest integration windows had been proposed to be up to 3 seconds after which the perceptual load of the naturalistic videos becomes too much to integrate ideas. Fairhall and colleagues (2014) found that low level features do not affect the perceptual integration window and proposed two mechanisms at play: a fast lower level processing to account for visual change and the higher level integration process window that takes up to 3 seconds. Our results suggest instead that low level feature integration windows can go up to 6 seconds. This difference could be due to statistical choices of considering longer windows (here we choose 40 second windows).

Instead, the functional connectivity of high level features show a sparse characterization. Sparse coding requires a large set of data and is achieved by an iterative non-linear process. At every iteration there is the application of weight vectors and error signals. In most models,

each neuron computes a product from the weight vector and input, it passes through a threshold, and the output along with the weight reproduces the input. The error is then fed as the input for the next iteration and keeps repeating till it reaches the optimal sparse code where only few neurons are left active (Sheridan et al, 2017). Recent advances in feedforward quantitative models like DNN and CNN have helped us capture and confirm this hierarchical multi-stage complexity of the spatio- temporal dynamics of the visual stream (Guclu, 2015). Here we utilized a pre-trained CNN and correlate it to MEG data in order to understand how the connectivity changes in the visual stream along the dorsal attention network in long intervals that are better able to characterize everyday experiences. We find that high level features are processed at later time intervals than low level features, and are represented sparsely as opposed to low level features.

## 5.3. Left vs right lateralization

In the second and third experiment (Chapters 3 and 4), using fMRI, we directly compare resting state and visual evoked data, first using still controlled images, and then using naturalistic videos. In order to do that we use the u90 method, a method that detects a minority of windows in resting state data with spatial information highly correlated to evoked data. This method capitalizes the importance of looking for scarce information following the sparse coding concept in higher order areas.

Our first study shows that the coherence between multivoxel representations of still hand stimuli and spontaneous fluctuations is in the left but not right somatomotor cortex. Instead in the second experiment, we find coherence between the visual representation of the common hand movement and spontaneous fluctuations in the right but not left somatomotor area. It is first important to highlight that these two experiments cannot be compared. While in the first experiment we used still images, in the second we use naturalistic videos with different types of movement. While in the first fMRI experiment we present controlled stimuli of still hands without any grasp shapes, in black and white, and with superimposed pink noise, in the second experiment we present naturalistic videos, controlled by counterbalancing across our different categories. However, both experiments study the encoding of visual information in the resting somatomotor area, and each show a lateralization on a different hemisphere.

Similar to our results with still images, LOTC activations of static still hands are overlapping with tool activations and connected selectively to the left premotor and intraparietal sulcus (Bracci et al., 2010; Bracci and Peelen, 2013; Lingnau and Downing,2015 ). Literature shows left lateralization activation when using the right dominant hand, however, a bilateral activation with the left hand (Kuhtz-Buschbeck et al., 2003; Schluter et al., 1998). Karolis and colleagues (2019) present a functional taxonomy of lateralization across 4 different axes: perception/action, emotion, communication, and decision making. They found that the principal components hands and fingers, with the highest loadings, activated the left hemisphere in the categories motor observation, touch, and finger tapping along the axis of action/perception. Kuhtz-Buschbeck and colleagues (2003) find that kinesthetic motor imagery activates the left premotor parietal and cerebellar regions, areas involved in motion. However this has some implications: though the hand stimuli were not suggestive of any movement, viewing hands evokes activity in motor related areas, the action observation system is still activated with still hands (Molinari, 2012) and the simulation and action observation networks are intertwined (Hardwick, 2018). This means that this effect could be on both sides of the brain and was not expected to be lateralized. It is worth noting that we see the same trend in the right somatomotor area and that we only had 19 subjects, suggesting that this effect could extend to the right hemisphere. Further experiments with a higher number of subjects that are both right handed and left handed should be able to shed more light on the lateralization effect.

Instead, in the fMRI experiment where subjects were viewing motion videos, the u90 analysis shows a right lateralized effect. These results are only with BOLD activations compared to resting state (u90), but not when comparing functional connectivity. Instead the functional connectivity shows differences in elaborating common vs uncommon hand motions in networks in both hemispheres. From the one hand, this could suggest that low frequency fluctuations have a different functional architecture where information is encoded in the left hemisphere (hands) to be utilized in the right hemisphere for further visuospatial elaboration (Mengotti, 2020). This could cause functional connectivity alterations on both sides of the brain. Another explanation could be due to the limitations of the U90 method itself that assumes the independence of every resting state time point instead of using clusters that could increase the effect or the power. Another approach to

study resting state is to report the main spatial clusters over time. Guitierez et al and colleagues (2019) find that a number of spatial patterns across the whole brain are repetitive and they report 6 main clusters. It would be interesting to apply this method and compare the main spatial clusters to evoked data to verify our results. However, this also highlights the importance of finding information in certain time windows of resting state as opposed to looking at any averaged data. The u90 method allows us to transparently measure spatial information. Even though we cannot explain the discrepancy between the lateralized results, this highlights the importance of taking holistic statistical approaches that look at both BOLD and FC. Future work in resting state should always consider both BOLD activations and FC approaches.

## 5.4. Role of spontaneous activity

It is not easy to understand the function of low level frequencies since even the biology behind them is still debated. One model views these frequencies organized, due to the natural synchrony of fast frequencies in large networks, where infra-slow frequencies would be simply summations of fast and local neural activity (Breakspear, 2017); in other words, they are a byproduct. However, this connectivity-synchrony model does not satisfy the drastic changes of infraslow activity in the wake state vs anesthesia (Mitra et al, 2015), nor yields good correlations with measured BOLD signals when simulated as low-pass filtered action potentials synchronized through known white-matter connections (Honey, et al., 2009). Alternatively, infra-slow frequencies could be a distinct organization with its own function and neurophysiology (Breakspear, 2017). Literature supporting a distinct process show infra-slow frequencies traveling along spatio-temporal trajectories in humans (Mitra et al., 2015) and mice (Matsui et al., 2016) in distinct cortical layers (Stroh et al., 2013) with dynamics that do not map on higher frequencies (Mitra, et al., 2018). Critically, these spontaneous patterns are not necessarily sensory-specific in sensory cortex or motor-specific in motor cortex, but may reflect more general patterns that are statistically associated during natural behavior and linked by structural-functional connections. For instance, regions of the visual cortex that respond to a specific visual category (bodies) also respond during reaching movements (Astafiev et al., 2004).

In this thesis, we interpret resting state activity as reflecting the history of coactivation of brain areas and networks creating a prior

architecture for the subsequent recruitment of task networks. In other words, it is creating a *prior* internal model of the environment (Betti et al., 2021). The brain represents everyday information in a sparse code manner in higher order areas. At rest, this information is found to be coded in a generic way (visual representation of the hand is stored in the resting somatomotor area even if it does not reflect low level features) and it reflects naturalistic everyday activity (FC of resting state LFF is more similar to evoked common LFF FC as opposed to uncommon). If there are not external stimuli, then prediction errors are not elicited. During this time, the brain might be reiterating the brain's priors (Lewis CM et al., 2009; Fiser J et al., 2010; Stoianov I et al., 2020). However, another function or explanation could be the optimization of models. If the brain is not receiving new incoming data for predictive error correction, two possible alternative optimization explanations could exist: 1) Pruning that is removing unnecessary information while maintaining accuracy, spontaneous activity then could be comparing complex models to pruned ones to select the most generic, or 2) generating data from a probabilistic model and then using it as real data to optimize further models.

Finally, slow waves have been suggested to be the neural correlates of thought since they are present both during wakefulness and sleep. Mind wandering and dreaming are both characterized with slow waves in the midcingulate (Lampros, 2017). In wake, slow waves are also prevalent in the premotor area which might explain why thoughts during wake have an organized logic as opposed to dreams that are social- content based. During sleep, we are disconnected from the environment so external stimuli do not affect the content of the dream; a similar phenomenon is observed with a reduction of cortical response during mind wandering. (Lampros, 2017). However, these sleep-like slow waves are also prevalent during mind blanking. The location of sleep-like slow waves can distinguish mind wandering from mind blanking, whereas the former is prevalent in the frontal area, the latter is in the posterior area (Andrillon, 2021). If all attentional lapses are characterized by slow waves, be it spontaneous thoughts, blanking, transitioning from wake to sleep, or sleeping, then one might argue that slow waves are more likely a characteristic of disconnection from the external world rather than a neural correlate of thought.

However, to understand the role of spontaneous low frequency fluctuations, we must first adopt an inside-out view of the brain

(Buzsaki, 2019). When trying to understand how perception and behavior are related, the classic view of the brain treats it as a receiver, reader, or experiencer of the external world and as such tries to assign stimulus associations with brain data. According to this view, the brain is passive and analyzes external stimuli for further action. Alternatively, from an inside-out perspective, the brain is made up of an internal structure where signals or frequencies already exist but acquire meaning by experiencing the world. This stresses an action-to-perception rather than a perception-to action framework. The 'outside in' framework is trying to assign representations or neural codes to outside stimuli, however building that dictionary is impossible. Instead, in the 'inside out' approach, the brain is trying to discover the world through action and assign meaning to neural codes that would otherwise be meaningless, by comparing how the brain output, reflected by action, influences incoming stimuli. The brain is not a *tabula rasa* that acquires information, but rather has predispositions and internal structures. In order to understand internally generated models, one must ask how they acquire meaning through action. Both during wakefulness and sleep, this internal model is being molded and changes with learning over time (rats, something about memory in sleep) reinforcing the role of them acting as priors; or in other words, an assigned meaning to a neural response that becomes a 'neural code' or an experience.

## Bibliography


Albert, N. B., Robertson, E. M., & Miall, R. C. (2009). The resting human brain and motor learning. Current Biology, 19(12), 1023-1027..

Aly, M., Chen, J., Turk-Browne, N. B., & Hasson, U. (2018). Learning naturalistic temporal structure in the posterior medial network. Journal of Cognitive Neuroscience, 30(9), 1345-1365.

Aly, M., Chen, J., Turk-Browne, N. B., & Hasson, U. (2018). Learning Naturalistic Temporal Structure in the Posterior Medial Network. Journal of cognitive neuroscience, 30(9), 1345–1365. https://doi.org/10.1162/jocn_a_01308

Amoruso, L., Finisguerra, A., & Urgesi, C. (2020). Spatial frequency tuning of motor responses reveals differential contribution of dorsal and ventral systems to action comprehension. Proceedings of the National Academy of Sciences of the United States of America, 117(23), 13151–13161. https://doi.org/10.1073/pnas.1921512117

Andersen, M., Björkman-Burtscher, I. M., Marsman, A., Petersen, E. T., & Boer, V. O. (2019). Improvement in diagnostic quality of structural and angiographic MRI of the brain using motion correction with interleaved, volumetric navigators. PloS One, 14(5), e0217145. doi:10.1371/journal.pone.0217145

Andersson, J. L., Hutton, C., Ashburner, J., Turner, R., & Friston, K. (2001). Modeling geometric deformations in EPI time series. NeuroImage, 13(5), 903–919. doi:10.1006/nimg.2001.0746

Andrillon, T., Burns, A., Mackay, T., Windt, J., & Tsuchiya, N. (2021). Predicting lapses of attention with sleep-like slow waves. Nature Communications, 12(1), 3657. doi:10.1038/s41467-021-23890-7

Association, W.M. (2013). World Medical Association Declaration of Helsinki: Ethical Principles for Medical Research Involving Human Subjects. Jama 310, 2191.

Astafiev, S. V., Stanley, C. M., Shulman, G. L., & Corbetta, M. (2004). Extrastriate body area in human occipital cortex responds to the performance of motor actions. Nature Neuroscience, 7(5),

542–548. doi:10.1038/nn1241

Averta, G., Valenza, G., Catrambone, V., Barontini, F., Scilingo, E. P., Bicchi, A., & Bianchi, M. (2019). On the time-invariance properties of upper limb synergies. IEEE Transactions on Neural Systems and Rehabilitation Engineering: A Publication of the IEEE Engineering in Medicine and Biology Society, 27(7), 1397–1406. doi:10.1109/TNSRE.2019.2918311

Baldassano, C., Chen, J., Zadbood, A., Pillow, J. W., Hasson, U., & Norman, K. A. (2017). Discovering event structure in continuous narrative perception and memory. Neuron, 95(3), 709-721.e5. doi:10.1016/j.neuron.2017.06.041

Baldassarre, A., Lewis, C. M., Committeri, G., Snyder, A. Z., Romani, G. L., & Corbetta, M. (2012). Individual variability in functional connectivity predicts performance of a perceptual task. Proceedings of the National Academy of Sciences, 109(9), 3516-3521.

Baldassarre, A., Ramsey, L. E., Siegel, J. S., Shulman, G. L., & Corbetta, M. (2016). Brain connectivity and neurological disorders after stroke. Current opinion in neurology, 29(6), 706–713. https://doi.org/10.1097/WCO.0000000000000396

Barlow, H. B. (1972). Single units and sensation: a neuron doctrine for perceptual psychology?. Perception, 1(4), 371-394.

Barnes, A., Bullmore, E. T., & Suckling, J. (2009). Endogenous human brain dynamics recover slowly following cognitive effort. PloS one, 4(8), e6626.

Bastos, A. M., Vezoli, J., Bosman, C. A., Schoffelen, J. M., Oostenveld, R., Dowdall, J. R., ... & Fries, P. (2015). Visual areas exert feedforward and feedback influences through distinct frequency channels. Neuron, 85(2), 390-401.

Belić, J. J., & Faisal, A. A. (2015). Decoding of human hand actions to handle missing limbs in neuroprosthetics. Frontiers in computational neuroscience, 9, 27.

Berger, H. (1929). Uber des Elektrenkephalogramm des Menschen, Arch. Psychiatr. Nervenkr., 87, 527-580

Berkes, P., Orbán, G., Lengyel, M., & Fiser, J. (2011). Spontaneous

cortical activity reveals hallmarks of an optimal internal model of the environment. Science (New York, N.Y.), 331(6013), 83–87. doi:10.1126/science.1195870

Betti, V., Corbetta, M., de Pasquale, F., Wens, V., & Della Penna, S. (2018). Topology of functional connectivity and hub dynamics in the beta band as temporal prior for natural vision in the human brain. Journal of Neuroscience, 38(15), 3858-3871.

Betti, V., Della Penna, S., de Pasquale, F., & Corbetta, M. (2021). Spontaneous beta band rhythms in the predictive coding of natural stimuli. The Neuroscientist: A Review Journal Bringing Neurobiology, Neurology and Psychiatry, 27(2), 184–201. doi:10.1177/1073858420928988

Betti, V., Della Penna, S., de Pasquale, F., Mantini, D., Marzetti, L., Romani, G. L., & Corbetta, M. (2013). Natural scenes viewing alters the dynamics of functional connectivity in the human brain. Neuron, 79(4), 782–797. https://doi.org/10.1016/j.neuron.2013.06.022

Beyeler, M., Rounds, E. L., Carlson, K. D., Dutt, N., & Krichmar, J. L. (2019). Neural correlates of sparse coding and dimensionality reduction. PLoS computational biology, 15(6), e1006908.

Bishop, G. (1993). Cyclic changes in excitability of the optic pathway of the rabbit. Am. J. Physiol., 103, 213-224

Biswal, B., Yetkin, FZ., Haughton, VM., Hyde, JS. (1995). Functional connectivity in the motor cortex of resting human brain using echo-planar mri. Magnet Reson Med, 34,537–541.

Blake, DT., Byl, NN., Merzenich, MM. (2002). Representation of the hand in the cerebral cortex. Behav Brain Res, 135,179–184.

Bracci, S., & Peelen, M. V. (2013). Body and object effectors: the organization of object representations in high-level visual cortex reflects body-object interactions. The Journal of Neuroscience: The Official Journal of the Society for Neuroscience, 33(46), 18247–18258. doi:10.1523/JNEUROSCI.1322-13.2013

Bracci, S., Ietswaart, M., Peelen, M. V., & Cavina-Pratesi, C. (2010). Dissociable neural responses to hands and non-hand body parts in human left extrastriate visual cortex. Journal of

Neurophysiology, 103(6), 3389–3397. doi:10.1152/jn.00215.2010

Brass, M., Schmitt, R. M., Spengler, S., & Gergely, G. (2007). Investigating action understanding: inferential processes versus action simulation. Current Biology: CB, 17(24), 2117–2121. doi:10.1016/j.cub.2007.11.057

Breakspear, M. (2017). Dynamic models of large-scale brain activity. Nature Neuroscience, 20(3), 340–352. doi:10.1038/nn.4497

Buccino, G., Lui, F., Canessa, N., Patteri, I., Lagravinese, G., Benuzzi, F., … Rizzolatti, G. (2004). Neural circuits involved in the recognition of actions performed by nonconspecifics: an FMRI study. Journal of Cognitive Neuroscience, 16(1), 114–126. doi:10.1162/089892904322755601

Burkhalter, A., Essen, DV. (1986). Processing of color, form and disparity information in visual areas VP and V2 of ventral extrastriate cortex in the macaque monkey. J Neurosci, 6, 2327–2351.

Buzsáki, G. (2019). The brain from inside out. Oxford University Press. https://doi.org/10.1093/oso/9780190905385.001.0001

Calvo-Merino, B., Glaser, D. E., Grèzes, J., Passingham, R. E., & Haggard, P. (2005). Action observation and acquired motor skills: an FMRI study with expert dancers. Cerebral Cortex (New York, N.Y.: 1991), 15(8), 1243–1249. doi:10.1093/cercor/bhi007

Cardellicchio, P., Hilt, P. M., Olivier, E., Fadiga, L., & D'Ausilio, A. (2018). Early modulation of intra-cortical inhibition during the observation of action mistakes. Scientific reports, 8(1), 1784.

Castiello, U., & Begliomini, C. (2008). The cortical control of visually guided grasping. The Neuroscientist : a review journal bringing neurobiology, neurology and psychiatry, 14(2), 157–170. https://doi.org/10.1177/1073858407312080

Cavanagh, S. E., Wallis, J. D., Kennerley, S. W., & Hunt, L. T. (2016). Autocorrelation structure at rest predicts value correlates of single neurons during reward-guided choice. eLife, 5. doi:10.7554/elife.18937

Chalk, M., Marre, O., & Tkačik, G. (2018). Toward a unified theory of efficient, predictive, and sparse coding. Proceedings of the

National Academy of Sciences, 115(1), 186-191.

Chan, AW-Y., Kravitz, DJ., Truong, S., Arizpe, J., Baker, CI. (2010). Cortical representations of bodies and faces are strongest in commonly experienced configurations. Nat Neurosci, 13, 417–418.

Chaudhuri, R., Knoblauch, K., Gariel, M.-A., Kennedy, H., & Wang, X.-J. (2015). A large-scale circuit mechanism for hierarchical dynamical processing in the primate cortex. Neuron, 88(2), 419–431. doi:10.1016/j.neuron.2015.09.008

Chen, J., Honey, C. J., Simony, E., Arcaro, M. J., Norman, K. A., & Hasson, U. (2016). Accessing real-life episodic information from minutes versus hours earlier modulates hippocampal and high-order cortical dynamics. Cerebral Cortex (New York, N.Y.: 1991), 26(8), 3428–3441. doi:10.1093/cercor/bhv155

Chouinard, PA., Paus, T. (2006). The Primary Motor and Premotor Areas of the Human Cerebral Cortex. Neurosci, 12, 143–152.

Churchland, M. M., Cunningham, J. P., Kaufman, M. T., Foster, J. D., Nuyujukian, P., Ryu, S. I., & Shenoy, K. V. (2012). Neural population dynamics during reaching. Nature, 487(7405), 51-56.

Cichy, R. M., Khosla, A., Pantazis, D., & Oliva, A. (2017). Dynamics of scene representations in the human brain revealed by magnetoencephalography and deep neural networks. NeuroImage, 153, 346-358.

Cichy, R. M., Pantazis, D., & Oliva, A. (2014). Resolving human object recognition in space and time. Nature neuroscience, 17(3), 455–462. https://doi.org/10.1038/nn.3635

Cirillo, R., Fascianelli, V., Ferrucci, L., & Genovesio, A. (2018). Neural intrinsic timescales in the macaque dorsal premotor cortex predict the strength of spatial response coding. iScience, 10, 203–210. doi:10.1016/j.isci.2018.11.033

Cole, M. W., Bassett, D. S., Power, J. D., Braver, T. S., & Petersen, S. E. (2014). Intrinsic and task-evoked network architectures of the human brain. Neuron, 83(1), 238-251.

Cox, RW. (1996). AFNI: Software for Analysis and Visualization of Functional Magnetic Resonance Neuroimages. Comput Biomed

Res, 29, 162–173.

Cunningham, J., Yu, B. (2014). Dimensionality reduction for large-scale neural recordings. Nat Neurosci 17, 1500–1509. https://doi.org/10.1038/nn.3776

de Pasquale, F., Della Penna, S., Snyder, A. Z., Lewis, C., Mantini, D., Marzetti, L., Belardinelli, P., Ciancetta, L., Pizzella, V., Romani, G. L., & Corbetta, M. (2010). Temporal dynamics of spontaneous MEG activity in brain networks. Proceedings of the National Academy of Sciences of the United States of America, 107(13), 6040–6045. https://doi.org/10.1073/pnas.0913863107

de Pasquale, F., Della Penna, S., Snyder, A. Z., Marzetti, L., Pizzella, V., Romani, G. L., & Corbetta, M. (2012). A cortical core for dynamic integration of functional networks in the resting human brain. Neuron, 74(4), 753-764.

Deco, G., Corbetta, M. (2011). The Dynamical Balance of the Brain at Rest. Neurosci, 17, 107–123.

Deco, G., Jirsa, V. K., & McIntosh, A. R. (2013). Resting brains never rest: computational insights into potential cognitive architectures. Trends in neurosciences, 36(5), 268–274. https://doi.org/10.1016/j.tins.2013.03.001

Della Penna, S., Delgratta, C., Granata, C., Pasquarelli, A., Pizzella, V., Rossi, R., Russo, M., Torquatiand, K., & Erné, S. N. (2000). Biomagnetic systems for clinical use. In Philosophical Magazine B (Vol. 80, Issue 5, pp. 937–948). Informa UK Limited. https://doi.org/10.1080/01418630008221960

Desmurget, M., Rossetti, Y., Jordan, M., Meckler, C., Prablanc, C. (1997). Viewing the hand prior to movement improves accuracy of pointing performed toward the unseen contralateral hand. Exp Brain Res, 115, 180–186.

Di Bono, M. G., Begliomini, C., Castiello, U., & Zorzi, M. (2015). Probing the reaching-grasping network in humans through multivoxel pattern decoding. Brain and Behavior, 5(11), e00412. doi:10.1002/brb3.412

Donner, T. H., Siegel, M., Oostenveld, R., Fries, P., Bauer, M., & Engel, A. K. (2007). Population activity in the human dorsal pathway

predicts the accuracy of visual motion detection. Journal of neurophysiology, 98(1), 345-359.

Ejaz, N., Hamada, M. & Diedrichsen, J. Hand use predicts the structure of representations in sensorimotor cortex. Nat Neurosci 18, 1034–1040 (2015). https://doi.org/10.1038/nn.4038

Engel, A. K., & Fries, P. (2010). Beta-band oscillations—signalling the status quo?. Current opinion in neurobiology, 20(2), 156-165.

Engel, AK., Fries, P., Singer, W. (2001). Dynamic predictions: Oscillations and synchrony in top–down processing. Nat Rev Neurosci, 2, 704–716.

Ernst, MO., Banks, MS. (2002). Humans integrate visual and haptic information in a statistically optimal fashion. Nature, 41, 429–433.

Errante, A., & Fogassi, L. (2019). Parieto-frontal mechanisms underlying observation of complex hand-object manipulation. Scientific Reports, 9(1), 348. doi:10.1038/s41598-018-36640-5

Fairhall, S. L., Albi, A., & Melcher, D. (2014). Temporal integration windows for naturalistic visual sequences. PloS One, 9(7), e102248. doi:10.1371/journal.pone.0102248

Fascianelli, V., Tsujimoto, S., Marcos, E., & Genovesio, A. (2019). Autocorrelation structure in the macaque dorsolateral, but not orbital or polar, prefrontal cortex predicts response-coding strength in a visually cued strategy task. Cerebral Cortex (New York, N.Y.: 1991), 29(1), 230–241. doi:10.1093/cercor/bhx321

Finn, E. S., Shen, X., Scheinost, D., Rosenberg, M. D., Huang, J., Chun, M. M., Papademetris, X., & Constable, R. T. (2015). Functional connectome fingerprinting: identifying individuals using patterns of brain connectivity. Nature neuroscience, 18(11), 1664–1671. https://doi.org/10.1038/nn.4135

Fiser, J., Berkes, P., Orbán, G., & Lengyel, M. (2010). Statistically optimal perception and learning: from behavior to neural representations. Trends in Cognitive Sciences, 14(3), 119–130. doi:10.1016/j.tics.2010.01.003

Fiser, J., Chiu, C., & Weliky, M. (2004). Small modulation of ongoing cortical dynamics by sensory input during natural vision.

Nature, 431(7008), 573-578.

Fonken, Y. M., Rieger, J. W., Tzvi, E., Crone, N. E., Chang, E., Parvizi, J., ... & Krämer, U. M. (2016). Frontal and motor cortex contributions to response inhibition: evidence from electrocorticography. Journal of neurophysiology, 115(4), 2224-2236.

Fonov, V., Evans, A., McKinstry, R., Almli, C., Collins, D. (2009). Unbiased nonlinear average age-appropriate brain templates from birth to adulthood. Neuroimage, 47, 102.

Fox, M. D., & Raichle, M. E. (2007). Spontaneous fluctuations in brain activity observed with functional magnetic resonance imaging. Nature reviews. Neuroscience, 8(9), 700–711. https://doi.org/10.1038/nrn2201

Fox, P., Raichle, M., Mintun, M., Dence, C. (1988). Nonoxidative glucose consumption during focal physiologic neural activity, Science, 241, 462-464

Galletti, C., and Fattori, P. (2003). Neuronal mechanisms for detection of motion in the field of view. Neuropsychologia, 41, 1717–1727

Gamberini M., Passarelli L., Fattori P., Zucchelli M., Bakola S., Luppino G., et al. (2009). Cortical connections of the visuomotor parietooccipital area V6Ad of the macaque monkey. J. Comp. Neurol., 513, 622–642 10.1002/cne.21980

Gardner, T., Goulden, N., & Cross, E. S. (2015). Dynamic modulation of the action observation network by movement familiarity. The Journal of Neuroscience: The Official Journal of the Society for Neuroscience, 35(4), 1561–1572. doi:10.1523/JNEUROSCI.2942-14.2015

Gibbon, J., Malapani, C., Dale, C. L., & Gallistel, C. R. (1997). Toward a neurobiology of temporal cognition: advances and challenges. Current opinion in neurobiology, 7(2), 170-184.

Gilboa, A., & Marlatte, H. (2017). Neurobiology of schemas and schema-mediated memory. Trends in cognitive sciences, 21(8), 618-631.

Glasser, M., Coalson, T., Robinson, E., Hacker, C., Harwell, J., Yacoub, E., Ugurbil, K., Andersson, J., Beckmann, CF., Jenkinson, M.,

Smith, SM., Essen, DCV. (2016). A multi-modal parcellation of human cerebral cortex. Nature, 536, 171–178.

Greicius, M., Krasnow, B., Reiss, A., Menon, V. (2003). Functional connectivity in the resting brain: a network analysis of the default mode hypothesis, Proc. Natl. Acad. Sci. U. S. A., 100, 253-258

Gruberger, M., Ben-Simon, E., Levkovitz, Y., Zangen, V., Hendler, T. (2011). Towards a neuroscience of mind-wandering, Front. Hum. Neurosci., 5, 56

Güçlü, U., & van Gerven, M. A. J. (2015). Deep neural networks reveal a gradient in the complexity of neural representations across the ventral stream. The Journal of Neuroscience: The Official Journal of the Society for Neuroscience, 35(27), 10005–10014. doi:10.1523/JNEUROSCI.5023-14.2015

Gutierrez-Barragan, D., Basson, M. A., Panzeri, S., & Gozzi, A. (2019). Infraslow state fluctuations govern spontaneous fMRI network dynamics. Current Biology: CB, 29(14), 2295-2306.e5. doi:10.1016/j.cub.2019.06.017

Hacker, C. D., Laumann, T. O., Szrama, N. P., Baldassarre, A., Snyder, A. Z., Leuthardt, E. C., & Corbetta, M. (2013). Resting state network estimation in individual subjects. Neuroimage, 82, 616-633.

Hacker, C. D., Snyder, A. Z., Pahwa, M., Corbetta, M., & Leuthardt, E. C. (2017). Frequency-specific electrophysiologic correlates of resting state fMRI networks. Neuroimage, 149, 446-457.

Hardwick, R. M., Caspers, S., Eickhoff, S. B., & Swinnen, S. P. (2018). Neural correlates of action: Comparing meta-analyses of imagery, observation, and execution. Neuroscience and Biobehavioral Reviews, 94, 31–44. doi:10.1016/j.neubiorev.2018.08.003

Hari, R., Forss, N., Avikainen, S., Kirveskari, E., Salenius, S., & Rizzolatti, G. (1998). Activation of human primary motor cortex during action observation: a neuromagnetic study. Proceedings of the National Academy of Sciences of the United States of America, 95(25), 15061–15065. doi:10.1073/pnas.95.25.15061

Hasson, U., Chen, J., & Honey, C. J. (2015). Hierarchical process

memory: memory as an integral component of information processing. Trends in Cognitive Sciences, 19(6), 304–313. doi:10.1016/j.tics.2015.04.006

Hasson, U., Yang, E., Vallines, I., Heeger, D. J., & Rubin, N. (2008). A hierarchy of temporal receptive windows in human cortex. The Journal of neuroscience : the official journal of the Society for Neuroscience, 28(10), 2539–2550. https://doi.org/10.1523/JNEUROSCI.5487-07.2008

Hauk, O., Johnsrude, I., Pulvermüller, F. (2004). Somatotopic Representation of Action Words in Human Motor and Premotor Cortex. Neuron, 41, 301–307.

Hesselmann, G., Kell, C. A., Eger, E., & Kleinschmidt, A. (2008). Spontaneous local variations in ongoing neural activity bias perceptual decisions. Proceedings of the National Academy of Sciences of the United States of America, 105(31), 10984–10989. https://doi.org/10.1073/pnas.0712043105

Holland, D., Kuperman, J. M., & Dale, A. M. (2010). Efficient correction of inhomogeneous static magnetic field-induced distortion in Echo Planar Imaging. NeuroImage, 50(1), 175–183. doi:10.1016/j.neuroimage.2009.11.044

Honey, C. J., Sporns, O., Cammoun, L., Gigandet, X., Thiran, J. P., Meuli, R., & Hagmann, P. (2009). Predicting human resting-state functional connectivity from structural connectivity. Proceedings of the National Academy of Sciences of the United States of America, 106(6), 2035–2040. doi:10.1073/pnas.0811168106

Honey, C. J., Thesen, T., Donner, T. H., Silbert, L. J., Carlson, C. E., Devinsky, O., Doyle, W. K., Rubin, N., Heeger, D. J., & Hasson, U. (2012). Slow cortical dynamics and the accumulation of information over long timescales. Neuron, 76(2), 423–434. https://doi.org/10.1016/j.neuron.2012.08.011

Hubel, D., Livingstone, M. (1987). Segregation of form, color, and stereopsis in primate area 18. J Neurosci 7, 3378–3415.

Hutchison, R. M., Womelsdorf, T., Allen, E. A., Bandettini, P. A., Calhoun, V. D., Corbetta, M., Della Penna, S., Duyn, J. H., Glover, G. H., Gonzalez-Castillo, J., Handwerker, D. A.,

Keilholz, S., Kiviniemi, V., Leopold, D. A., de Pasquale, F., Sporns, O., Walter, M., & Chang, C. (2013). Dynamic functional connectivity: promise, issues, and interpretations. NeuroImage, 80, 360–378. https://doi.org/10.1016/j.neuroimage.2013.05.079

Huth, A. G., Nishimoto, S., Vu, A. T., & Gallant, J. L. (2012). A continuous semantic space describes the representation of thousands of object and action categories across the human brain. Neuron, 76(6), 1210-1224.

Huxley, T. (1884). An Introduction to the Study of Zoology Illustrated by the Crayfish, D. Appleton & Company, New York

Iacoboni, M., Koski, L. M., Brass, M., Bekkering, H., Woods, R. P., Dubeau, M. C., Rizzolatti, G. (2001). Reafferent copies of imitated actions in the right superior temporal cortex. Proceedings of the National Academy of Sciences of the United States of America, 98(24), 13995–13999. doi:10.1073/pnas.241474598

Ingram, J. N., Körding, K. P., Howard, I. S., & Wolpert, D. M. (2008). The statistics of natural hand movements. Experimental Brain Research, 188(2), 223–236. doi:10.1007/s00221-008-1355-3

Iriki, A., Tanaka, M., Iwamura, Y. (1996). Coding of modified body schema during tool use by macaque postcentral neurones. NeuroReport, 2325–2330.

Jenkinson, N., & Brown, P. (2011). New insights into the relationship between dopamine, beta oscillations and motor function. Trends in neurosciences, 34(12), 611-618.

Jensen, O., & Mazaheri, A. (2010). Shaping functional architecture by oscillatory alpha activity: Gating by inhibition. Frontiers in Human Neuroscience, 4, Article 186. https://doi.org/10.3389/fnhum.2010.00186

Jensen, O., Bonnefond, M., Marshall, T. R., & Tiesinga, P. (2015). Oscillatory mechanisms of feedforward and feedback visual processing. In Trends in Neurosciences (Vol. 38, Issue 4, pp. 192–194). Elsevier BV. https://doi.org/10.1016/j.tins.2015.02.006

Karolis, V., Corbetta, M., Schotten, MT. (2019). The architecture of functional lateralisation and its relationship to callosal

connectivity in the human brain. Nat Commun 10, 1417.

Kennett, S., Taylor-Clarke, M., Haggard, P. (2001). Noninformative vision improves the spatial resolution of touch in humans. Curr Biol, 11, 1188–1191.

Kety, S., Schmidt, C. (1948). The nitrous oxide method for the quantitative determination of cerebral blood flow in man: theory, procedure and normal values J. Clin. Investig., 27, 107-119

Kilner, J. M., Paulignan, Y., & Blakemore, S. J. (2003). An interference effect of observed biological movement on action. Current Biology: CB, 13(6), 522–525. doi:10.1016/s0960-9822(03)00165-9

Kim, D., Livne, T., Metcalf, N. V., Corbetta, M., & Shulman, G. L. (2020). Spontaneously emerging patterns in human visual cortex and their functional connectivity are linked to the patterns evoked by visual stimuli. Journal of Neurophysiology, 124(5), 1343–1363. doi:10.1152/jn.00630.2019

Klaes, C., Kellis, S., Aflalo, T., Lee, B., Pejsa, K., Shanfield, K., Hayes-Jackson, S., Aisen, M., Heck, C., Liu, C., Andersen, RA. (2015). Hand Shape Representations in the Human Posterior Parietal Cortex. J Neurosci, 35, 15466–15476.

Kleiner, M., Brainard, D., Pelli, D., Ingling, A., Murray, R., Broussard, C. (2007). What's new in psychtoolbox-3. Perception, 36, 1–16.

Klimesch, W., Sauseng, P., & Hanslmayr, S. (2007). EEG alpha oscillations: the inhibition-timing hypothesis. Brain research reviews, 53(1), 63–88. https://doi.org/10.1016/j.brainresrev.2006.06.003

Kloosterman, N. A., Meindertsma, T., Hillebrand, A., van Dijk, B. W., Lamme, V. A., & Donner, T. H. (2015). Top-down modulation in human visual cortex predicts the stability of a perceptual illusion. Journal of neurophysiology, 113(4), 1063-1076.

Koch, G., Cercignani, M., Pecchioli, C., Versace, V., Oliveri, M., Caltagirone, C., … Bozzali, M. (2010). In vivo definition of parieto-motor connections involved in planning of grasping movements. NeuroImage, 51(1), 300–312. doi:10.1016/j.neuroimage.2010.02.022

Kolasinski, J., Makin, T. R., Jbabdi, S., Clare, S., Stagg, C. J., & Johansen-Berg, H. (2016). Investigating the stability of fine-grain digit somatotopy in individual human participants. Journal of Neuroscience, 36(4), 1113-1127.

Kolers, P. A., & Von Grunau, M. (1977). Fixation and Attention in Apparent Motion. Quarterly Journal of Experimental Psychology, 29(3), 389-395. https://doi.org/10.1080/14640747708400616

Kuehn, E., Haggard, P., Villringer, A., Pleger, B., Sereno, M. (2018). Visually-Driven Maps in Area 3b. J Neurosci, 38, 1295–1310.

Kuhtz-Buschbeck, J., Mahnkopf, C., Holzknecht, C., Siebner, H., Ulmer, S., Jansen, O. (2003). Effector-independent representations of simple and complex imagined finger movements: a combined fMRI and TMS study. Eur J Neurosci, 18, 3375–3387.

Lawrence, D. G., & Hopkins, D. A. (1976). The development of motor control in the rhesus monkey: evidence concerning the role of corticomotoneuronal connections. Brain: A Journal of Neurology, 99(2), 235–254. doi:10.1093/brain/99.2.235

Lee, J. H., Whittington, M. A., & Kopell, N. J. (2013). Top-down beta rhythms support selective attention via interlaminar interaction: a model. PLoS computational biology, 9(8), e1003164.

Leo, A., Handjaras, G., Bianchi, M., Marino, H., Gabiccini, M., Guidi, A., ... & Ricciardi, E. (2016). A synergy-based hand control is encoded in human motor cortical areas. Elife, 5, e13420.

Lerner, Y., Honey, C. J., Silbert, L. J., & Hasson, U. (2011). Topographic mapping of a hierarchy of temporal receptive windows using a narrated story. The Journal of neuroscience : the official journal of the Society for Neuroscience, 31(8), 2906–2915. https://doi.org/10.1523/JNEUROSCI.3684-10.2011

Lescroart, M. D., & Gallant, J. L. (2019). Human scene-selective areas represent 3D configurations of surfaces. Neuron, 101(1), 178-192.

Lewis, C. M., Baldassarre, A., Committeri, G., Romani, G. L., & Corbetta, M. (2009). Learning sculpts the spontaneous activity of the resting human brain. Proceedings of the National

Academy of Sciences of the United States of America, 106(41), 17558–17563. doi:10.1073/pnas.0902455106

Lingnau, A., & Downing, P. E. (2015). The lateral occipitotemporal cortex in action. Trends in Cognitive Sciences, 19(5), 268–277. doi:10.1016/j.tics.2015.03.006

Livingstone, M., & Hubel, D. (1988). Segregation of form, color, movement, and depth: anatomy, physiology, and perception. Science (New York, N.Y.), 240(4853), 740–749. https://doi.org/10.1126/science.3283936

Livne, T., Kim, D., Metcalf, N. V., Shulman, G. L., & Corbetta, M. (2020). Spontaneous emergence of behaviorally relevant motifs in human motor cortex. doi:10.1101/2020.10.25.353326

Livne, T., Kim, D., Metcalf, N. V., Zhang, L., Pini, L., Shulman, G. L., & Corbetta, M. (2022). Spontaneous activity patterns in human motor cortex replay evoked activity patterns for hand movements. Scientific Reports, 12(1), 16867. doi:10.1038/s41598-022-20866-5

Longo, MR., Azañón, E., Haggard, P. (2010). More than skin deep: Body representation beyond primary somatosensory cortex. Neuropsychologia, 48, 655–668.

Longo, MR., Betti, V., Aglioti, SM., Haggard, P. (2009). Visually Induced Analgesia: Seeing the Body Reduces Pain. J Neurosci, 29, 12125–12130.

Longo, MR., Haggard, P. (2010). An implicit body representation underlying human position sense. Proc National Acad Sci, 107, 11727–11732.

Lynch, L. K., Lu, K.-H., Wen, H., Zhang, Y., Saykin, A. J., & Liu, Z. (2018). Task-evoked functional connectivity does not explain functional connectivity differences between rest and task conditions. Human Brain Mapping, 39(12), 4939–4948. doi:10.1002/hbm.24335

Ma, L., Narayana, S., Robin, D. A., Fox, P. T., & Xiong, J. (2011). Changes occur in resting state network of motor system during 4 weeks of motor skill learning. NeuroImage, 58(1), 226–233. https://doi.org/10.1016/j.neuroimage.2011.06.014

Mantini, D., Della Penna, S., Marzetti, L., de Pasquale, F., Pizzella, V., Corbetta, M., & Romani, G. L. (2011). A signal-processing pipeline for magnetoencephalography resting-state networks. Brain connectivity, 1(1), 49–59. https://doi.org/10.1089/brain.2011.0001

Marco-Pallarés, J., Münte, T. F., & Rodríguez-Fornells, A. (2015). The role of high-frequency oscillatory activity in reward processing and learning. Neuroscience & Biobehavioral Reviews, 49, 1-7.

Marzetti, L., Della Penna, S., Snyder, A. Z., Pizzella, V., Nolte, G., de Pasquale, F., ... & Corbetta, M. (2013). Frequency specific interactions of MEG resting state activity within and across brain networks as revealed by the multivariate interaction measure. Neuroimage, 79, 172-183.

Matsui, T., Murakami, T., & Ohki, K. (2016). Transient neuronal coactivations embedded in globally propagating waves underlie resting-state functional connectivity. Proceedings of the National Academy of Sciences of the United States of America, 113(23), 6556–6561. doi:10.1073/pnas.1521299113

Mengotti, P., Käsbauer, A.-S., Fink, G. R., & Vossel, S. (2020). Lateralization, functional specialization, and dysfunction of attentional networks. Cortex; a Journal Devoted to the Study of the Nervous System and Behavior, 132, 206–222. doi:10.1016/j.cortex.2020.08.022

Merzenich, MM., Kaas, JH., Sur, M., Lin, C. (1978). Double representation of the body surface within cytoarchitectonic area 3b and 1 in "SI" in the owl monkey (aotus trivirgatus). J Comp Neurol, 181, 41–73.

Michalareas, G., Vezoli, J., Van Pelt, S., Schoffelen, J. M., Kennedy, H., & Fries, P. (2016). Alpha-beta and gamma rhythms subserve feedback and feedforward influences among human visual cortical areas. Neuron, 89(2), 384-397.

Miller, J. E., Ayzenshtat, I., Carrillo-Reid, L., & Yuste, R. (2014). Visual stimuli recruit intrinsically generated cortical ensembles. Proceedings of the National Academy of Sciences of the United States of America, 111(38), E4053–E4061. https://doi.org/10.1073/pnas.1406077111

Mitra, A., Kraft, A., Wright, P., Acland, B., Snyder, A. Z., Rosenthal, Z., … Raichle, M. E. (2018). Spontaneous infra-slow brain activity has unique spatiotemporal dynamics and laminar structure. Neuron, 98(2), 297-305.e6. doi:10.1016/j.neuron.2018.03.015

Mitra, A., Kraft, A., Wright, P., Acland, B., Snyder, A. Z., Rosenthal, Z., Czerniewski, L., Bauer, A., Snyder, L., Culver, J., Lee, J. M., & Raichle, M. E. (2018). Spontaneous Infra-slow Brain Activity Has Unique Spatiotemporal Dynamics and Laminar Structure. Neuron, 98(2), 297–305.e6. https://doi.org/10.1016/j.neuron.2018.03.015

Molinari, E., Baraldi, P., Campanella, M., Duzzi, D., Nocetti, L., Pagnoni, G., & Porro, C. A. (2013). Human parietofrontal networks related to action observation detected at rest. Cerebral Cortex (New York, N.Y.: 1991), 23(1), 178–186. doi:10.1093/cercor/bhr393

Monfardini, E., Gazzola, V., Boussaoud, D., Brovelli, A., Keysers, C., & Wicker, B. (2013). Vicarious neural processing of outcomes during observational learning. PloS One, 8(9), e73879. doi:10.1371/journal.pone.0073879

Murata, A., Gallese, V., Luppino, G., Kaseda, M., & Sakata, H. (2000). Selectivity for the shape, size, and orientation of objects for grasping in neurons of monkey parietal area AIP. Journal of Neurophysiology, 83(5), 2580–2601. doi:10.1152/jn.2000.83.5.2580

Murray, J. D., Bernacchia, A., Freedman, D. J., Romo, R., Wallis, J. D., Cai, X., … Wang, X.-J. (2014). A hierarchy of intrinsic timescales across primate cortex. Nature Neuroscience, 17(12), 1661–1663. doi:10.1038/nn.3862

Nieto-Castanon, A. (2020). Handbook of functional connectivity Magnetic Resonance Imaging methods in CONN. Boston, MA: Hilbert Press

Nishida, S., Tanaka, T., Shibata, T., Ikeda, K., Aso, T., & Ogawa, T. (2014). Discharge-rate persistence of baseline activity during fixation reflects maintenance of memory-period activity in the macaque posterior parietal cortex. Cerebral Cortex (New York, N.Y.: 1991), 24(6), 1671–1685. doi:10.1093/cercor/bht031

Ogawa, T., & Komatsu, H. (2010). Differential temporal storage capacity in the baseline activity of neurons in macaque frontal eye field and area V4. Journal of Neurophysiology, 103(5), 2433–2445. doi:10.1152/jn.01066.2009

Oldfield R. C. (1971). The assessment and analysis of handedness: the Edinburgh inventory. Neuropsychologia, 9(1), 97–113. https://doi.org/10.1016/0028-3932(71)90067-4

Olshausen, B. A., & Field, D. J. (2004). Sparse coding of sensory inputs. Current opinion in neurobiology, 14(4), 481-487.

Olshausen, B. A., & Rozell, C. J. (2017). Sparse codes from memristor grids. Nature Nanotechnology, 12(8), 722-723.

Orgs, G., Dovern, A., Hagura, N., Haggard, P., Fink, GR., Weiss, PH. (2016). Constructing Visual Perception of Body Movement with the Motor Cortex. Cereb Cortex, 26, 440–449.

Penfield, Boldrey (1937). Somatic motor and sensory representation in the cerebral cortex of main as studied by electrical stimulation. Brain, 60, 389–443.

Perogamvros, L., Baird, B., Seibold, M., Riedner, B., Boly, M., & Tononi, G. (2017). The phenomenal contents and neural correlates of spontaneous thoughts across wakefulness, NREM sleep, and REM sleep. Journal of Cognitive Neuroscience, 29(10), 1766–1777. doi:10.1162/jocn_a_01155

Pezzulo, G., Zorzi, M., Corbetta, M. (2021). The secret life of predictive brains: what's spontaneous activity for? Trends Cogn Sci 25, 730–743.

Piantoni, G., Kline, K. A., & Eagleman, D. M. (2010). Beta oscillations correlate with the probability of perceiving rivalrous visual stimuli. Journal of Vision, 10(13), 18-18.

Porro, CA., Francescato, MP., Cettolo, V., Diamond, ME., Baraldi, P., Zuiani, C., Bazzocchi, M., Prampero, PE. (1996). Primary Motor and Sensory Cortex Activation during Motor Performance and Motor Imagery: A Functional Magnetic Resonance Imaging Study. J Neurosci, 16, 7688–7698.

Power, JD., Barnes, KA., Snyder, AZ., Schlaggar, BL., Petersen, SE. (2012). Spurious but systematic correlations in functional

connectivity MRI networks arise from subject motion. Neuroimage, 59, 2142–2154.

Raichle, M., MacLeod, A., Snyder, A., Powers, W., Gusnard, D., Shulman, G. (2001). A default mode of brain function, Proc. Natl. Acad. Sci. U. S. A., 98, 676-682

Raichle, M., Mintun, M. (2006). Brain work and brain imaging, Annu. Rev. Neurosci., 29, 449-476

Raichle, ME. (2011). The Restless Brain. Brain Connectivity, 1, 3–12.

Raos, V., Umiltá, M.-A., Gallese, V., & Fogassi, L. (2004). Functional properties of grasping-related neurons in the dorsal premotor area F2 of the macaque monkey. Journal of Neurophysiology, 92(4), 1990–2002. doi:10.1152/jn.00154.2004

Raposo, A., Moss, HE., Stamatakis, EA., Tyler, LK. (2009). Modulation of motor and premotor cortices by actions, action words and action sentences. Neuropsychologia, 47, 388–396.

Rassi, E., Wutz, A., Müller-Voggel, N., & Weisz, N. (2019). Prestimulus feedback connectivity biases the content of visual experiences. Proceedings of the National Academy of Sciences, 116(32), 16056-16061.

Rizzolatti, G., Luppino, G. (2001). The Cortical Motor System. Neuron, 31,889–901.

Romano, D., Mioli, A., D'Alonzo, M., Maravita, A., Lazzaro, VD., Pino, GD. (2021). Behavioral and Physiological Evidence of a favored Hand Posture in the Body Representation for Action. Cereb Cortex, 31, 3299–3310.

Rosenke, M., van Hoof, R., van den Hurk, J., Grill-Spector, K., & Goebel, R. (2021). A probabilistic functional atlas of human occipito-temporal visual cortex. Cerebral Cortex (New York, N.Y.: 1991), 31(1), 603–619. doi:10.1093/cercor/bhaa246

Rushworth, MFS., Krams, M., Passingham, RE. (2001). The Attentional Role of the Left Parietal Cortex: The Distinct Lateralization and Localization of Motor Attention in the Human Brain. J Cognitive Neurosci, 13, 698–710.

Samann, P., Wehrle, R., Hoehn, D., Spoormaker, V., Peters, H., Tully, C., Holsboer, F., Czisch, M. (2011). Development of the brain's

default mode network from wakefulness to slow wave sleep, Cereb. cortex, 21,2082-

Sauseng, P., Klimesch, W., Stadler, W., Schabus, M., Doppelmayr, M., Hanslmayr, S., ... & Birbaumer, N. (2005). A shift of visual spatial attention is selectively associated with human EEG alpha activity. European journal of neuroscience, 22(11), 2917-2926.

Schieber, MH. (2001). Constraints on Somatotopic Organization in the Primary Motor Cortex. J Neurophysiol, 86, 2125–2143.

Schluter, N. (1998). Temporary interference in human lateral premotor cortex suggests dominance for the selection of movements. A study using transcranial magnetic stimulation. Brain: A Journal of Neurology, 121(5), 785–799. doi:10.1093/brain/121.5.785

Schurz, M., Maliske, L., & Kanske, P. (2020). Cross-network interactions in social cognition: A review of findings on task related brain activation and connectivity. Cortex; a Journal Devoted to the Study of the Nervous System and Behavior, 130, 142–157. doi:10.1016/j.cortex.2020.05.006

Sebastiani, V., de Pasquale, F., Costantini, M., Mantini, D., Pizzella, V., Romani, G. L., & Della Penna, S. (2014). Being an agent or an observer: different spectral dynamics revealed by MEG. Neuroimage, 102, 717-728.

Shadlen, M. N., & Newsome, W. T. (1998). The variable discharge of cortical neurons: implications for connectivity, computation, and information coding. The Journal of neuroscience : the official journal of the Society for Neuroscience, 18(10), 3870–3896. https://doi.org/10.1523/JNEUROSCI.18-10-03870.1998

Sheridan, P. M., Cai, F., Du, C., Ma, W., Zhang, Z., & Lu, W. D. (2017). Sparse coding with memristor networks. Nature Nanotechnology, 12(8), 784–789. doi:10.1038/nnano.2017.83

Shimada, S. (2010). Deactivation in the sensorimotor area during observation of a human agent performing robotic actions. Brain and Cognition, 72(3), 394–399. doi:10.1016/j.bandc.2009.11.005

Simon, K. C., Nadel, L., & Payne, J. D. (2022). The functions of sleep: A cognitive neuroscience perspective. PNAS, 119(44),

e2201795119. https://doi.org/10.1073/pnas.2201795119

Simoncelli, EP., Olshausen, BA. (2001). Natural image statistics and neural representation. Annu Rev Neurosci, 24, 1193–1216.

Simony, E., Honey, C. J., Chen, J., Lositsky, O., Yeshurun, Y., Wiesel, A., & Hasson, U. (2016). Dynamic reconfiguration of the default mode network during narrative comprehension. Nature Communications, 7(1), 12141. doi:10.1038/ncomms12141

Smith, S. M., Nichols, T. E., Vidaurre, D., Winkler, A. M., Behrens, T. E., Glasser, M. F., Ugurbil, K., Barch, D. M., Van Essen, D. C., & Miller, K. L. (2015). A positive-negative mode of population covariation links brain connectivity, demographics and behavior. Nature neuroscience, 18(11), 1565–1567. https://doi.org/10.1038/nn.4125

Snyder, A., Raichle, M. (2012). A brief history of the resting state: The Washington University perspective, NeuroImage, 62(2). https://doi.org/10.1016/j.neuroimage.2012.01.044.

Sonkusare, S., Breakspear, M., & Guo, C. (2019). Naturalistic stimuli in neuroscience: Critically acclaimed. Trends in Cognitive Sciences, 23(8), 699–714. doi:10.1016/j.tics.2019.05.004

Spadone, S., Betti, V., Sestieri, C., Pizzella, V., Corbetta, M., & Della Penna, S. (2021). Spectral signature of attentional reorienting in the human brain. NeuroImage, 244, 118616. https://doi.org/10.1016/j.neuroimage.2021.118616

Spadone, S., Penna, SD., Sestieri, C., Betti, V., Tosoni, A., Perrucci, MG., Romani, GL., Corbetta, M. (2015). Dynamic reorganization of human resting-state networks during visuospatial attention. Proc National Acad Sci, 112, 8112–8117.

Spitzer, B., & Haegens, S. (2017). Beyond the status quo: A role for beta oscillations in endogenous content (RE)activation. ENeuro. Society for Neuroscience.

Stevens, J. A., Fonlupt, P., Shiffrar, M., & Decety, J. (2000). New aspects of motion perception. Neuroreport, 11(1), 109–115. doi:10.1097/00001756-200001170-00022

Stoianov, I., Maisto, D., & Pezzulo, G. (2020). The hippocampal formation as a hierarchical generative model supporting

generative replay and continual learning. doi:10.1101/2020.01.16.908889

Strappini, F., Wilf, M., Karp, O., Goldberg, H., Harel, M., Furman-Haran, E., … Malach, R. (2019). Resting-state activity in high-order visual areas as a window into natural human brain activations. Cerebral Cortex (New York, N.Y.: 1991), 29(9), 3618–3635. doi:10.1093/cercor/bhy242

Strigaro, G., Ruge, D., Chen, J., Marshall, L., Desikan, M., Cantello, R., Rothwell, JC. (2015). Interaction between visual and motor cortex: a transcranial magnetic stimulation study. J Physiology, 593, 2365–2377.

Stringer, C., Pachitariu, M., Steinmetz, N., Reddy, CB., Carandini, M., Harris, KD. (2019). Spontaneous behaviors drive multidimensional, brainwide activity. Science, 364, 7893.

Stroh, A., Adelsberger, H., Groh, A., Rühlmann, C., Fischer, S., Schierloh, A., … Konnerth, A. (2013). Making waves: Initiation and propagation of corticothalamic Ca2+ waves in vivo. Neuron, 77(6), 1136–1150. doi:10.1016/j.neuron.2013.01.031

Tai, Y. F., Scherfler, C., Brooks, D. J., Sawamoto, N., & Castiello, U. (2004). The human premotor cortex is 'mirror' only for biological actions. Current Biology: CB, 14(2), 117–120. doi:10.1016/j.cub.2004.01.005

Taubert, M., Lohmann, G., Margulies, D. S., Villringer, A., & Ragert, P. (2011). Long-term effects of motor training on resting-state networks and underlying brain structure. NeuroImage, 57(4), 1492–1498. https://doi.org/10.1016/j.neuroimage.2011.05.078

Tomasi, D., Wang, G. J., & Volkow, N. D. (2013). Energetic cost of brain functional connectivity. Proceedings of the National Academy of Sciences of the United States of America, 110(33), 13642–13647. https://doi.org/10.1073/pnas.1303346110

Turella, L., Wurm, M. F., Tucciarelli, R., & Lingnau, A. (2013). Expertise in action observation: recent neuroimaging findings and future perspectives. Frontiers in Human Neuroscience, 7, 637. doi:10.3389/fnhum.2013.00637

Van Kerkoerle, T., Self, M. W., Dagnino, B., Gariel-Mathis, M. A., Poort, J., Van Der Togt, C., & Roelfsema, P. R. (2014). Alpha and

gamma oscillations characterize feedback and feedforward processing in monkey visual cortex. Proceedings of the National Academy of Sciences, 111(40), 14332-14341.

Van Kesteren, M. T., Ruiter, D. J., Fernández, G., & Henson, R. N. (2012). How schema and novelty augment memory formation. Trends in neurosciences, 35(4), 211-219.

von Stein, A., & Sarnthein, J. (2000). Different frequencies for different scales of cortical integration: From local gamma to long range alpha/theta synchronization. International Journal of Psychophysiology, 38(3), 301–313. https://doi.org/10.1016/S0167-8760(00)00172-0

Wang, Z., Chen, LM., Négyessy, L., Friedman, RM., Mishra, A., Gore, JC., Roe, AW. (2013). The Relationship of Anatomical and Functional Connectivity to Resting-State Connectivity in Primate Somatosensory Cortex. Neuron, 78, 1116–1126.

Weiss, S., & Mueller, H. M. (2012). "Too many betas do not spoil the broth": the role of beta brain oscillations in language processing. Frontiers in psychology, 3, 201.

Wen, W., Haggard, P. (2020). Prediction error and regularity detection underlie two dissociable mechanisms for computing the sense of agency. Cognition, 195, 104074.

Wens, V. (2015). Investigating complex networks with inverse models: analytical aspects of spatial leakage and connectivity estimation. Physical Review E, 91(1), 012823.

Wens, V., Marty, B., Mary, A., Bourguignon, M., Op de Beeck, M., Goldman, S., ... & De Tiege, X. (2015). A geometric correction scheme for spatial leakage effects in MEG/EEG seed‐based functional connectivity mapping. Human brain mapping, 36(11), 4604-4621.

Willems, RM., Hagoort, P., Casasanto, D. (2009). Body-Specific Representations of Action Verbs. Psychol Sci, 21, 67–74.

Wilson, T. D., Dunn, D. S., Kraft, D., & Lisle, D. J. (1989). Introspection, attitude change, and attitude-behavior consistency: The disruptive effects of explaining why we feel the way we do. In Advances in experimental social psychology (Vol. 22, pp. 287-343). Academic Press.

Wolpert, D. M., & Ghahramani, Z. (2000). Computational principles of movement neuroscience. Nature neuroscience, 3 Suppl, 1212–1217. https://doi.org/10.1038/81497

World Medical Association. (2013). World Medical Association Declaration of Helsinki: ethical principles for medical research involving human subjects. JAMA: The Journal of the American Medical Association, 310(20), 2191–2194. doi:10.1001/jama.2013.281053

Yao, H., Shi, L., Han, F., Gao, H., Dan, Y. (2007). Rapid learning in cortical coding of visual scenes. Nat Neurosci, 10, 772–778.

Yeo, B. T., Krienen, F. M., Sepulcre, J., Sabuncu, M. R., Lashkari, D., Hollinshead, M., Roffman, J. L., Smoller, J. W., Zöllei, L., Polimeni, J. R., Fischl, B., Liu, H., & Buckner, R. L. (2011). The organization of the human cerebral cortex estimated by intrinsic functional connectivity. Journal of neurophysiology, 106(3), 1125–1165. https://doi.org/10.1152/jn.00338.2011

Zhang, L., Pini, L., Kim, D., Shulman, G. L., & Corbetta, M. (2023). Spontaneous activity patterns in human attention networks code for hand movements. The Journal of Neuroscience: The Official Journal of the Society for Neuroscience, 43(11), 1976–1986. doi:10.1523/JNEUROSCI.1601-22.2023